

# First Principle Research on Ga Rich GaAs<sub>0.5</sub>P<sub>0.5</sub>(001) $\beta_2(4\times 2)$ and As(P) rich $\beta_2(2\times 4)$ Reconstruction Surfaces With and Without Cs Adsorption

**Siyi He**

NUIST: Nanjing University of Information Science and Technology <https://orcid.org/0000-0002-3509-927X>

**Mingzhu Yang** (✉ [ymznuist16@126.com](mailto:ymznuist16@126.com))

NUIST: Nanjing University of Information Science and Technology

**Shixin Pei**

NUIST: Nanjing University of Information Science and Technology

---

## Research Article

**Keywords:** GaAs<sub>0.5</sub>P<sub>0.5</sub>(001), Ga rich Ga rich  $\beta_2(4\times 2)$  reconstruction surface, As(P) rich  $\beta_2(2\times 4)$  reconstruction surface, work function, Mulliken charge, dipole moment.

**Posted Date:** April 26th, 2021

**DOI:** <https://doi.org/10.21203/rs.3.rs-265102/v1>

**License:**   This work is licensed under a Creative Commons Attribution 4.0 International License.

[Read Full License](#)

---

# First principle research on Ga rich GaAs<sub>0.5</sub>P<sub>0.5</sub>(001) $\beta_2(4\times 2)$ and As(P) rich $\beta_2(2\times 4)$ reconstruction surfaces with and without Cs adsorption

Siyi He, Mingzhu Yang\*, Shixin Pei

School of Physics and Optoelectronic Engineering, Nanjing University of Information Science and Technology, Nanjing, 210044

\*Corresponding author: Tel: +86 18013885873; E-mail: ymznuist16@126.com

**Abstracts:** Based on first principle calculations, Ga rich and As(P) rich clean GaAs<sub>0.5</sub>P<sub>0.5</sub>(001) reconstruction surfaces and adsorbed surfaces with 0.125ML coverage of Cs at different sites are researched. Formation energy of Ga rich GaAs<sub>0.5</sub>P<sub>0.5</sub>(001)  $\beta_2(4\times 2)$  reconstruction surface is smaller than that of As(P) rich one, and the work functions of Ga rich  $\beta_2(4\times 2)$  and As(P) rich  $\beta_2(2\times 4)$  surfaces are 4.657 eV and 5.187 eV, respectively. The adsorption energies of Cs adatoms on both surfaces are negative, showing that Cs adsorption is a stable exothermic process. The work functions of two surfaces both decrease after Cs adsorption, and the average variation of As(P) rich  $\beta_2(2\times 4)$  surface is larger. Mulliken charge analysis shows that Cs adatoms transfer electrons to GaAsP substrate, resulting in Cs-GaAsP dipoles which lower the work functions. When Cs atoms are located at D<sub>2</sub> of Ga rich surface and D<sub>2</sub>' of As(P) rich surface, work function values of the two reconstruction surfaces reach the minimums, which are 2.834eV and 2.859eV, respectively. By calculating dipole moments, it can be found that Cs adatoms on the topmost layer form larger effective dipole moments with GaAsP substrate than the Cs atoms located in the trench.

**Keywords:** GaAs<sub>0.5</sub>P<sub>0.5</sub>(001); Ga rich  $\beta_2(4\times 2)$  reconstruction surface; As(P) rich  $\beta_2(2\times 4)$  reconstruction surface; work function; Mulliken charge; dipole moment

## Declarations

This study was funded by National Natural Science Foundation of China (Grant Nos. 61705108) and Natural Science Foundation of Jiangsu Province (Grant No. BK20170959).

The authors declare that they have no known competing financial interests or personal relationships that could have appeared to influence the work reported in this paper.

The datasets used or analyzed during the current study are available from the corresponding author on reasonable request.

## 1. Introduction

GaAs<sub>1-x</sub>P<sub>x</sub> is a ternary III-V compound semiconductor with the bandgap varying from 1.42eV (in GaAs) to 2.26eV (in GaP)<sup>[1]</sup>. In recent years, it has attracted wide attention in electronic devices, such as Light Emitting Diode (LED)<sup>[2,3]</sup>, photocathodes<sup>[4-7]</sup>, solar cells<sup>[8]</sup>, and so on. As we know, the blue-green light (450-570 nm) is an important way to communicate in the ocean, because the loss of the blue-green light transferring in the seawater is very low and the transmission efficient is high<sup>[9,10]</sup>. To satisfy the need of ocean exploration, ocean communications, and under-sea imaging, GaAsP photocathodes with short cutoff wavelength and high quantum efficiency at blue-green light spectra were prepared by adjusting P component in GaAs photocathodes<sup>[4-7]</sup>. Jiao *et al* prepared a transmission-mode (t-mode) Al<sub>0.7</sub>Ga<sub>0.3</sub>As<sub>0.9</sub>P<sub>0.1</sub>/GaAs<sub>0.9</sub>P<sub>0.1</sub> photocathode by molecular beam epitaxy(MBE), and the GaAsP sample possesses a quantum efficiency peak of 62% at 560 nm, and the quantum efficiency at 532nm is 59%<sup>[4]</sup>. By using metal-organic chemical vapor deposition (MOCVD), Hamamatsu *et al* prepared t-mode GaAsP photocathodes of which the peak quantum efficiency is 52% at 520nm<sup>[6]</sup>. All the above mentioned GaAsP photocathodes were activated by Cs atoms firstly to get zero electron affinity(ZEA) and secondly by Cs, O alternative adsorption to get negative electron affinity(NEA) surfaces., which are essential for photoelectrons to escape from the photocathodes.

As the same as other III-arsenic, GaAs<sub>1-x</sub>P<sub>x</sub> belongs to Fm3m space group, and it is in cubic zinc blende form at ambient conditions<sup>[1]</sup>. Theoretical and experimental results about surfaces of III-V cubic semiconductors are abundant, mainly focusing on GaAs(001) reconstruction surfaces<sup>[11-15]</sup>. Due to different epitaxial methods and cation/anion ratios, GaAs(001) surface present a series of reconstruction ranging from As-rich  $c(4\times 4)$ <sup>[13]</sup>,  $\alpha(2\times 4)$ <sup>[12,13]</sup>,  $\alpha_2(2\times 4)$ <sup>[12,13]</sup>,  $\beta(2\times 4)$ <sup>[12,13]</sup>,  $\beta_2(2\times 4)$ <sup>[12,13]</sup> to Ga rich  $\beta_2(4\times 2)$ <sup>[12-14]</sup> and  $\zeta(4\times 2)$ <sup>[15]</sup>. For GaP(001) surface, the above mentioned reconstruction styles were also observed using Low Energy Electron Diffraction (LEED)<sup>[16]</sup> and Scanning Tunneling Microscopy (STM)<sup>[17]</sup>, and were theoretically researched by density function theory (DFT)<sup>[18]</sup>. Among the various reconstruction forms, As(P) rich  $\beta_2(2\times 4)$  and Ga rich  $\beta_2(4\times 2)$  reconstruction

surfaces are the most popular ones.

Meanwhile, for GaAsP, either theoretical or experimental researches on reconstruction surfaces are rare, nor are the researches about Cs adsorption on GaAsP surfaces. In this paper, Ga rich  $\beta_2(4\times 2)$  and As(P) rich  $\beta_2(2\times 4)$  reconstruction surface models were built, and surface formation energies, surface morphology, Mulliken population, and work function were obtained and discussed based on first-principle calculations. Then Cs adsorption models with different adsorption sites based on the two clean surfaces were built and calculated. Cs induced surface reconstruction and relaxation, Mulliken population redistribution, and dipole moments were discussed. This work would provide some theoretical guidance for the preparation and activation of GaAsP photocathodes.

## 2. Method of Calculations

The top view and side view of Ga rich GaAs<sub>0.5</sub>P<sub>0.5</sub>(001)  $\beta_2(4\times 2)$  and As(P) rich GaAs<sub>0.5</sub>P<sub>0.5</sub>(001)  $\beta_2(2\times 4)$  reconstruction surfaces are shown in Fig. 1. Ga rich GaAs<sub>0.5</sub>P<sub>0.5</sub>(001)  $\beta_2(4\times 2)$  reconstruction surface consists of two repeated Ga-Ga dimers in the topmost layer and one Ga-Ga dimer in the trench where a pair of As(P) atoms are missing. Similarly, As(P) rich GaAs<sub>0.5</sub>P<sub>0.5</sub>(001)  $\beta_2(2\times 4)$  reconstruction surface consists of two repeated As-P dimers on top and one As-P dimer in the trench in which a pair of Ga atoms were removed. The two reconstruction surfaces were modeled by using periodic supercells, in which a vacuum of 12Å were added. To make it more convenient to observe the changes in the model, along with the consideration of the calculation error and symmetry, five bilayers were built in all. So there are 36 Ga atoms, 15 As atoms, and 15 P atoms in an unit supercell of Ga rich  $\beta_2(4\times 2)$  surface model while there are 30 Ga atoms, 18 As atoms, and 18 P atoms in an unit supercell of As(P) rich  $\beta_2(2\times 4)$  surface model. The surface dangling bonds at the bottom layer are saturated with fractionally charged pseudohydrogens. The atoms in the two lowest bilayers were kept frozen at bulk configuration to simulate bulk condition while the atoms in the top layers were relaxed freely.

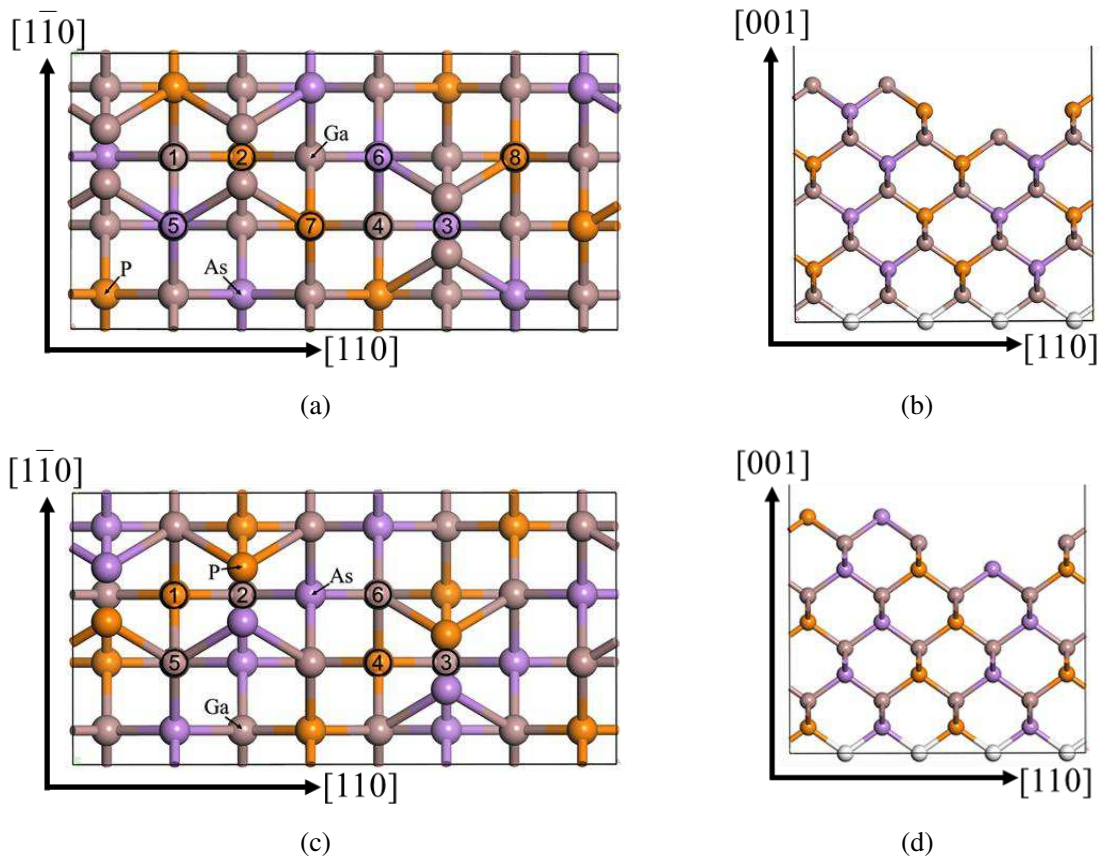


Fig. 1. GaAs<sub>0.5</sub>P<sub>0.5</sub>(001) reconstruction surfaces (a) top view of Ga rich GaAs<sub>0.5</sub>P<sub>0.5</sub>(001)  $\beta_2(4 \times 2)$  (b) side view of Ga rich GaAs<sub>0.5</sub>P<sub>0.5</sub>(001)  $\beta_2(4 \times 2)$  (c) top view of As(P) rich GaAs<sub>0.5</sub>P<sub>0.5</sub>(001)  $\beta_2(2 \times 4)$  (d) side view of As(P) rich GaAs<sub>0.5</sub>P<sub>0.5</sub>(001)  $\beta_2(2 \times 4)$

Cs adsorption on Ga rich  $\beta_2(4 \times 2)$  surface and As(P) rich  $\beta_2(2 \times 4)$  surface are discussed respectively. In this paper, eight adsorption sites were chosen on the Ga rich surface, while six adsorption sites were chosen on the As(P) rich one. The chosen adsorption sites are shown in Fig. 1 with circled numbers.  $D_m$  is adopted to describe the adsorption site when a Cs atom adsorbs on dimers, and  $T_n$  is adopted if the adsorption site is the top of an atom. The corner mark  $m$  or  $n$  corresponds to the number in Fig. 1. The eight sites on the Ga rich surface are respectively described as  $T_1$ ,  $D_2$ ,  $D_3$ ,  $T_4$ ,  $T_5$ ,  $T_6$ ,  $T_7$ , and  $T_8$  in the following contents. While the six sites on the As rich surface are respectively described as  $T_1'$ ,  $D_2'$ ,  $D_3'$ ,  $T_4'$ ,  $T_5'$ , and  $T_6'$ .

The general calculations were carried out with DFT utilizing Cambridge Sequential Total Energy Package (CASTEP) codes<sup>[19]</sup>. The Broyden-Fletcher-Goldfarb-Shanno (BFGS) algorithm was adopted to optimize the surface models. The exchange-correlation potential

was treated by the generalized gradient approximation (GGA) parameterized by Perdew-Burke-Ernzerhof (PBE)<sup>[20,21]</sup>. The atomic pseudopotential was expressed by using ultrasoft pseudopotential. The integral in the Brillouin zone was sampled with the Monkhorst Pack scheme<sup>[22]</sup>. Ga: 3d<sup>10</sup>4s<sup>2</sup>4p<sup>1</sup>, As: 4s<sup>2</sup>4p<sup>3</sup>, and P: 3s<sup>2</sup>3p<sup>3</sup> were taken into calculation as valence electrons. The k-point was set as 4×4×1 with a cutoff energy of 400eV.

### 3. Results and Discussion

#### 3.1 Clean Surfaces

Surface formation energy, which reflects the stability of a surface, can be calculated as follows<sup>[23]</sup>:

$$\sigma = (E_{slab}^{tot} - nE_{bulk} - N_H \mu_H) / A \quad (1)$$

where  $E_{slab}^{tot}$  represents the total energy of the slab,  $n$  represents the number of conventional cells in the slab,  $A$  represents the area of the surface,  $N_H$  represents the number of H atoms,  $\mu_H$  represents the energy of H atoms in the surface model.

As the ratio of cation and anion is not 1 in either Ga rich  $\beta_2(4 \times 2)$  surface or As rich  $\beta_2(2 \times 4)$  surface, Eq. (1) is revised as follows:

$$\sigma A = E_{slab}^{tot} - N_{Ga} \mu_{Ga} - N_{As} \mu_{As} - N_P \mu_P - N_H \mu_H \quad (2)$$

where  $N_{Ga}$ ,  $N_{As}$ , and  $N_P$  stand for the number of Ga, As, and P atoms, respectively;  $\mu_{Ga}$ ,  $\mu_{As}$ , and  $\mu_P$  stand for the energy of Ga, As and P atoms in the bulk, respectively. In both types of surface,  $N_{Ga}$ ,  $N_{As}$ , and  $N_P$  are bounded by  $N_{As} = N_P$ ; additionally  $N_{Ga} > N_{As} + N_P$  in Ga rich surface and  $N_{Ga} < N_{As} + N_P$  in As(P) rich surface. Assuming the whole environmental keeps in thermodynamic equilibrium state,  $\mu_{Ga}$ ,  $\mu_{As}$  and  $\mu_P$  are not independent, but constrained by the following relation:

$$\mu_{Ga} + 0.5\mu_{As} + 0.5\mu_P = E_{bulk} \quad (3)$$

Since the number of the atoms is certain,  $\sigma$  is only determined by  $\mu_{Ga}$ .

$$\sigma A = E_{slab}^{tot} - 2N_{As}E_{bulk} - (N_{Ga} - 2N_{As})\mu_{Ga} - 8\mu_H \quad (4)$$

Fig. 2 shows the surface energy curves of the two GaAs<sub>0.5</sub>P<sub>0.5</sub>(001) reconstruction surfaces.  $\Delta\mu_{Ga}$  means the difference of the energy of Ga atoms in the reconstruction surfaces and that in the bulk. The negative  $\Delta\mu_{Ga}$  means As(P) rich condition while positive one means Ga rich condition. Results show that the formation energy of Ga rich  $\beta_2(4 \times 2)$  surface descends as  $\Delta\mu_{Ga}$  increases, and it is always negative, showing that this reconstruction form is stable. Meanwhile, the formation energy of As(P) rich  $\beta_2(2 \times 4)$  surface ascends as  $\Delta\mu_{Ga}$  increases. And the formation energy is negative under As(P) rich condition while it is positive under Ga rich condition, demonstrating that As(P) rich  $\beta_2(2 \times 4)$  surface is only stable under As(P) rich condition.

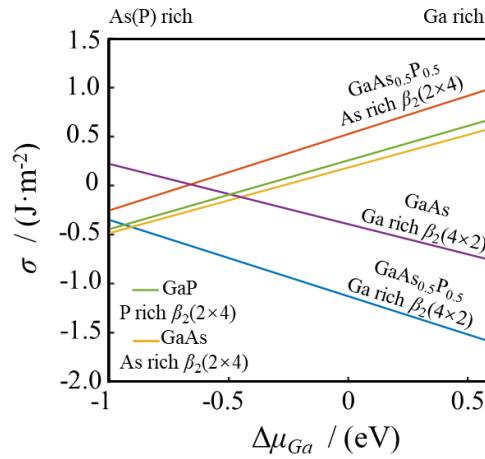


Fig. 2. Formation energy curves of GaAs<sub>0.5</sub>P<sub>0.5</sub>(001) reconstruction surfaces

For comparison, the formation energy curves of GaAs(001)  $\beta_2(2 \times 4)$ , GaAs(001)  $\beta_2(4 \times 2)$  and GaP (001)  $\beta_2(2 \times 4)$  reconstruction surfaces were added in Fig. 2<sup>[11]</sup>. It can be found that the surface formation energy of Ga rich GaAs<sub>0.5</sub>P<sub>0.5</sub> (001)  $\beta_2(4 \times 2)$  reconstruction surface is lower than that of pure GaAs at whole range, and the average energy of As(P) rich GaAs<sub>0.5</sub>P<sub>0.5</sub> reconstruction surface is higher than that of pure GaAs and pure GaP.

For semiconductors, work function is the minimum energy that the electrons inside the semiconductor require to escape into the external. It can be calculated by the following formula<sup>[24]</sup>:

$$\Phi = E_{vac} - E_f \quad (5)$$

where  $E_{vac}$  is the vacuum energy and  $E_f$  is Fermi level. The calculated work function of Ga rich  $\beta_2(4 \times 2)$  reconstruction surface is 4.657 eV, while that of As rich  $\beta_2(2 \times 4)$  reconstruction surface is 5.187 eV.

The calculated Mulliken charge distribution of the atoms in the topmost and second bilayers are shown in Table. 1. As a comparison, the Mulliken charge of Ga, P, and As atoms in bulk  $\text{GaAs}_{0.5}\text{P}_{0.5}$  are 0.29, -0.40, and -0.19, respectively. The calculated Mulliken charge of atoms in the third, fourth, and lower bilayers vary slightly. Meanwhile, those of Ga atoms decrease significantly, especially in the first bilayers. Without doubt, this phenomenon is very common for type-3 surface<sup>[23,25]</sup>, in which cations and anions appear tier upon tier and there are dangling bonds in the topmost layer. By making a thorough research, it can be found that the population of Ga 3d state electrons remain the same substantially, and electrons in Ga 4p state decreases, while those in Ga 4s state increases. As to anions, Mulliken charge difference of P and As atoms is obvious, showing that the electronegativity of P atom is larger. As a whole, As 4p state and P 3p state decreases, while those in P 3s state increases. The number of electrons in As 4s state does not vary significantly.

Table. 1. Mulliken charge distribution of atoms in the topmost and second bilayers of Ga rich clean surface

First bilayer			Second bilayer					
Atom	Total	Charge	Atom	Total	Charge	Atom	Total	Charge
Ga <sub>1-1</sub>	12.92	0.08	Ga <sub>2-1</sub>	12.80	0.20	P <sub>2-1</sub>	5.38	-0.38
Ga <sub>1-2</sub>	12.92	0.08	Ga <sub>2-2</sub>	12.88	0.12	P <sub>2-2</sub>	5.36	-0.36
Ga <sub>1-3</sub>	12.93	0.07	Ga <sub>2-3</sub>	12.88	0.12	P <sub>2-3</sub>	5.38	-0.38
Ga <sub>1-4</sub>	12.92	0.08	Ga <sub>2-4</sub>	12.7	0.30	P <sub>2-4</sub>	5.37	-0.37
P <sub>1-1</sub>	5.41	-0.41	Ga <sub>2-5</sub>	12.85	0.15	As <sub>2-1</sub>	4.99	0.01
P <sub>1-2</sub>	5.38	-0.38	Ga <sub>2-6</sub>	12.9	0.10	As <sub>2-2</sub>	5.04	-0.04
P <sub>1-3</sub>	5.38	-0.38	Ga <sub>2-7</sub>	12.88	0.12	As <sub>2-3</sub>	5.08	-0.08
As <sub>1-1</sub>	5.26	-0.26	Ga <sub>2-8</sub>	12.91	0.09	As <sub>2-4</sub>	5.09	-0.09

As <sub>1-2</sub>	5.27	-0.27
As <sub>1-3</sub>	5.26	-0.26

The Mulliken charge distribution of atoms in the topmost and second bilayers of As(P) rich surface is shown in Table 2. Compared with the second bilayer, the Mulliken charge distribution of atoms in the first bilayer is much more different from that of bulk. More specifically, absolute charge value of As atoms and P atoms decrease significantly, because the total number of covalent bonds of these four atoms drop. As a result, the charge of Ga adjacent atoms is much smaller than that in bulk. As to Ga atoms in the second bilayer, Mulliken charge values of Ga<sub>2-5</sub>, Ga<sub>2-6</sub>, Ga<sub>2-7</sub>, and Ga<sub>2-8</sub> are smaller than those of the other four Ga atoms, mainly because they are neighbors of As(P) atoms which have dangling bonds.

Table. 2. Mulliken charge distribution of atoms in the topmost and second bilayers of As(P) rich clean surface

First bilayer			Second bilayer					
Atom	Total	Charge	Atom	Total	Charge	Atom	Total	Charge
As <sub>1-1</sub>	5.12	-0.12	As <sub>2-1</sub>	5.09	-0.09	Ga <sub>2-1</sub>	12.64	0.36
As <sub>1-2</sub>	5.12	-0.12	As <sub>2-2</sub>	5.14	-0.14	Ga <sub>2-2</sub>	12.64	0.36
P <sub>1-1</sub>	5.26	-0.27	As <sub>2-3</sub>	5.19	-0.19	Ga <sub>2-3</sub>	12.64	0.36
P <sub>1-2</sub>	5.27	-0.27	As <sub>2-4</sub>	5.14	-0.14	Ga <sub>2-4</sub>	12.64	0.36
Ga <sub>1-1</sub>	12.94	0.06	P <sub>2-1</sub>	5.36	-0.36	Ga <sub>2-5</sub>	12.78	0.22
Ga <sub>1-2</sub>	12.85	0.16	P <sub>2-2</sub>	5.39	-0.39	Ga <sub>2-6</sub>	12.84	0.16
Ga <sub>1-3</sub>	12.94	0.06	P <sub>2-3</sub>	5.30	-0.29	Ga <sub>2-7</sub>	12.82	0.18
Ga <sub>1-4</sub>	12.86	0.15	P <sub>2-4</sub>	5.39	-0.39	Ga <sub>2-8</sub>	12.80	0.20
Ga <sub>1-5</sub>	12.86	0.15						
Ga <sub>1-6</sub>	12.84	0.17						

After geometry optimization, thicknesses of bilayers ( $D$ ) and distances between adjacent bilayers ( $d$ ) of Ga rich and As(P) rich reconstruction surfaces are shown in Table 3. As the lower layers were fixed during geometry optimization,  $d_{34}$  and  $D_4$  represent the data of bulk, and the thicknesses of lower bilayers and distances between lower adjacent

bilayers remain the same as well. The thicknesses of first bilayers and the distances between the first and the second bilayers in both surfaces vary significantly. For the Ga rich clean surface, the thickness of first bilayer is much smaller than that of bulk, because the outermost Ga atoms which lose the upper attraction force move close to their As(P) neighbors. For the same reason, As(P) atoms which lose some of Ga neighbors move downwards. As a result, the distance between first and second bilayers drops. Meanwhile, it is very different in As(P) rich clean surface, in which the thickness of first bilayer increase while the distance between the first and second bilayers decrease. In fact, the mechanism is the same as that in Ga rich surface. The Ga atoms which lose As(P) neighbors in the first bilayer move downwards to achieve new stability, and this relaxation plays a more important role than the outermost As(P) atoms. As a result, the first bilayer gets thicker. The average bond-length of Ga-P is 2.373 Å, Ga-As is 2.434 Å, respectively in the bulk. For the Ga rich clean surface, the average bond-length of Ga-P is 2.390 Å, Ga-As is 2.442 Å, respectively. As the average bond lengths ascends slightly, the average bond population descends.

Table. 3. Thicknesses of bilayers and distances between adjacent bilayers of Ga rich and As(P) rich reconstruction surfaces

Layer	Thickness / Distance	
	Ga rich clean surface	As(P) rich clean surface
$D_1$	0.907 Å	1.889 Å
$d_{12}$	1.133 Å	0.924 Å
$D_2$	1.670 Å	1.745 Å
$d_{23}$	1.351 Å	1.184 Å
$D_3$	1.446 Å	1.540 Å
$d_{34}$	1.388 Å	1.388 Å
$D_4$	1.388 Å	1.388 Å

The total density of states (TDOS) and partial density of states (PDOS) of GaAs<sub>0.5</sub>P<sub>0.5</sub> bulk and GaAs<sub>0.5</sub>P<sub>0.5</sub>(001) reconstruction surfaces are shown in Fig. 3. It is illustrated that in contrast to the bulk the TDOS curve of the Ga rich  $\beta_2(4\times 2)$  surface shifts to lower energy

significantly, while that of the As rich  $\beta_2(2\times 4)$  surface shifts not evidently. The TDOS of both reconstruction surfaces is not zero at Fermi level. In the Ga rich model, electrons of Ga 4s, 4p state, As 4p state and P 3p state play the main role, while in the As(P) rich model, it is mainly affected by electrons of As 4s, 4p state and P 3p state.

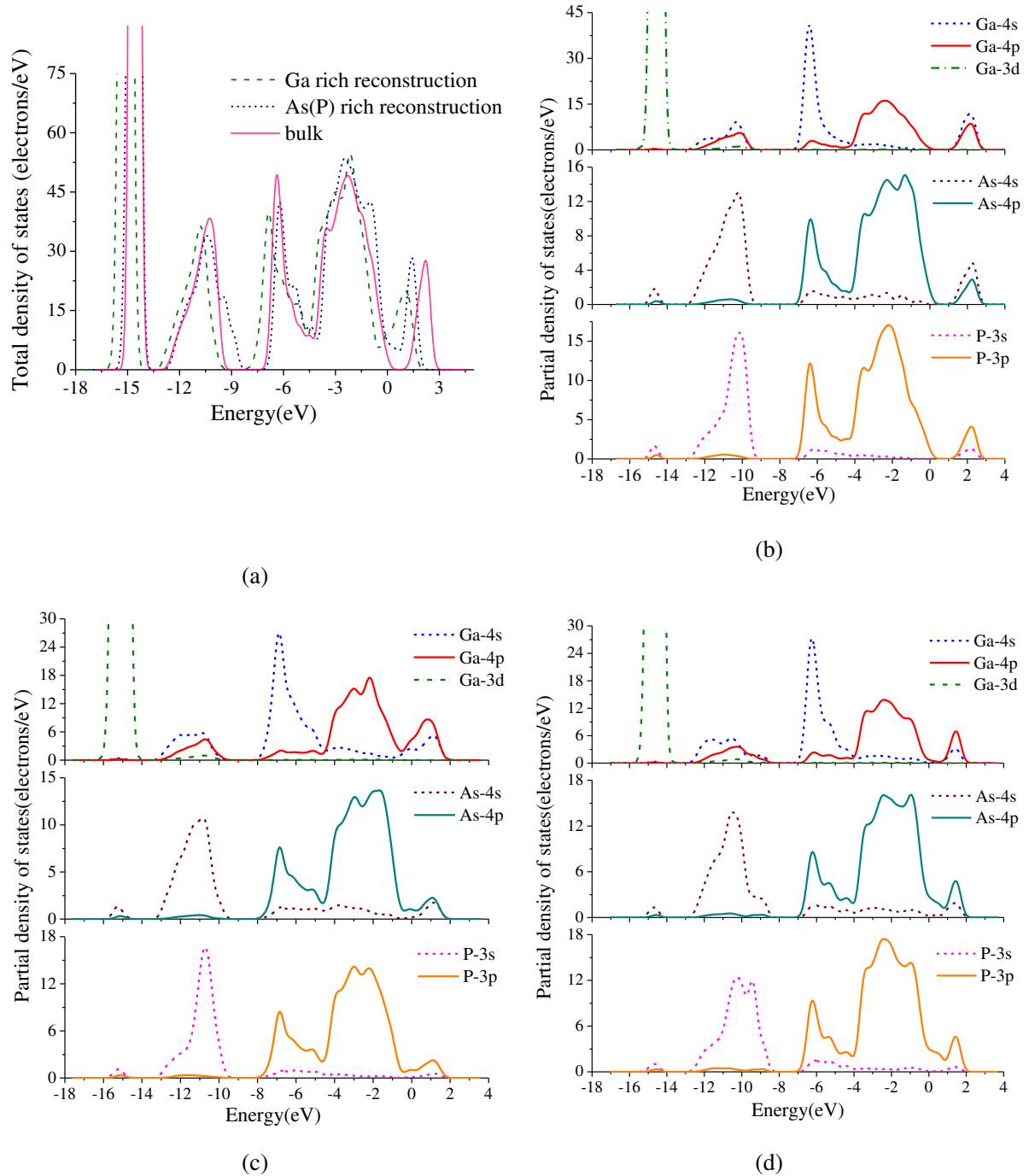


Fig. 3. TDOS and PDOS of GaAs<sub>0.5</sub>P<sub>0.5</sub> bulk and GaAs<sub>0.5</sub>P<sub>0.5</sub>(001) reconstruction surfaces (a) TDOS curves of GaAs<sub>0.5</sub>P<sub>0.5</sub> bulk and GaAs<sub>0.5</sub>P<sub>0.5</sub>(001) reconstruction surfaces (b) PDOS curves of GaAs<sub>0.5</sub>P<sub>0.5</sub>

bulk (c) PDOS curves of Ga rich  $\text{GaAs}_{0.5}\text{P}_{0.5}(001) \beta_2(4 \times 2)$  (d) PDOS curves of As(P) rich  $\text{GaAs}_{0.5}\text{P}_{0.5}(001) \beta_2(2 \times 4)$

### 3.2 Cs adsorption on the reconstruction surfaces

Adsorption energy can be calculated by the following formula<sup>[26]</sup>:

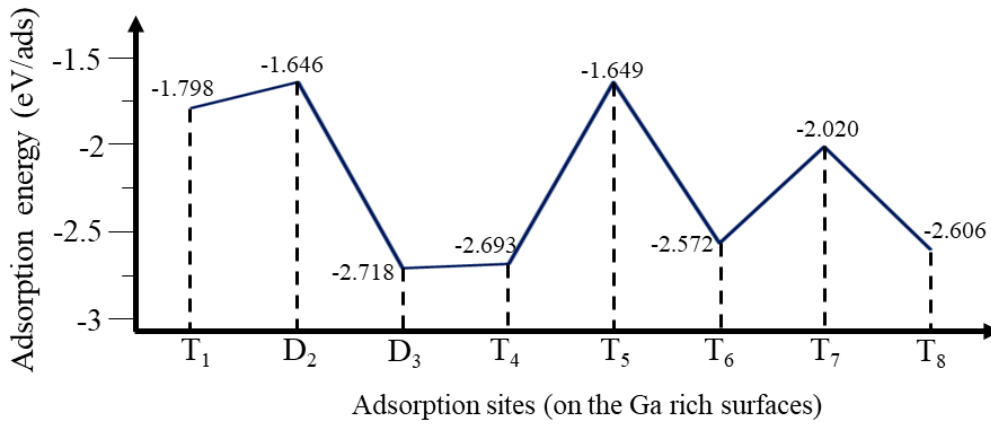
$$E_{ads} = \frac{E_{tot} - (E_{orig} + nE_i)}{n} \quad (6)$$

where  $E_{orig}$  represents the total energy of the structure before adsorption is made,  $E_i$  represents the energy of the adsorption adatom,  $E_{tot}$  represents the total energy of the structure after adsorption is made, and  $n$  is the total number of the adsorption adatoms. In this paper,  $n$  equals to 1, and  $E_i$  stands for the energy of a Cs atom, so the Eq. (6) is revised as follows:

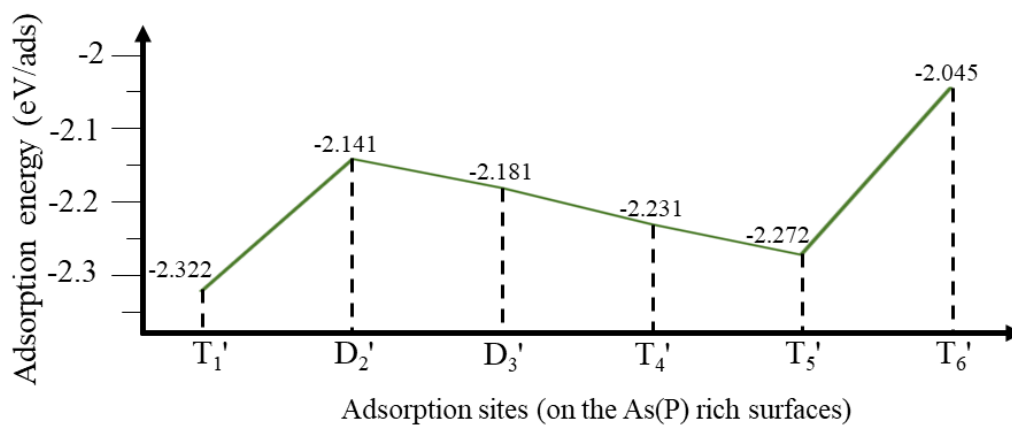
$$E_{ads} = E_{tot} - (E_{orig} + E_{Cs}) \quad (7)$$

The calculated adsorption energies and the work function values of all adsorption sites on both reconstruction surfaces are shown in Fig. 4. and Fig. 5.

From Fig. 4, it can be found that the adsorption energies of Cs adatom are all negative, showing that Cs adsorption is an exothermic process and the new systems are stable. The most energetically favored sites on Ga rich surface are  $D_3$  and  $T_4$ , followed by  $T_6$ , while  $T_1'$  and  $T_5'$  on As(P) rich surface are the most favored ones.

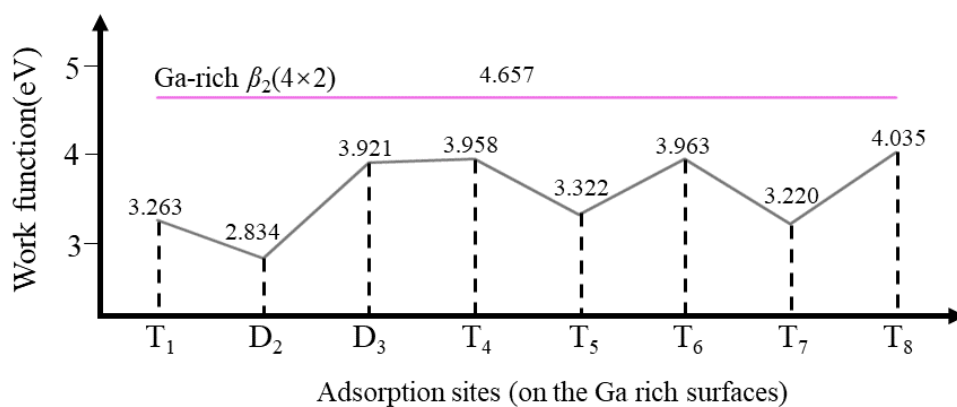


(a)

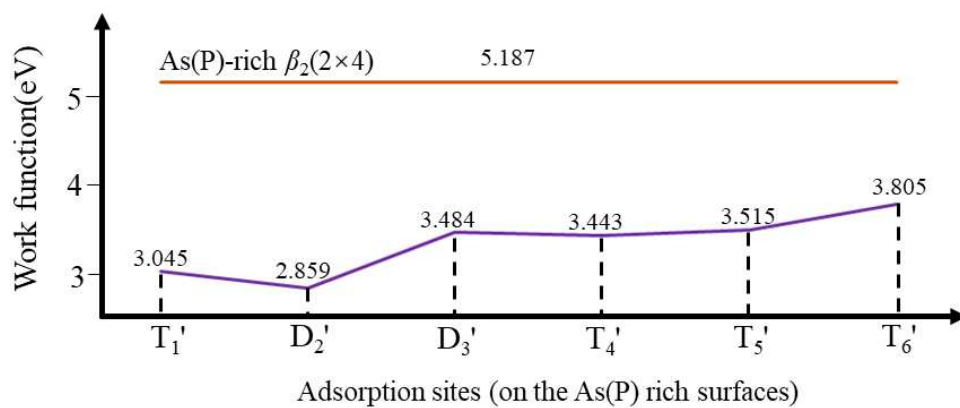


(b)

Fig. 4. Cs adsorption energies of the two reconstruction surfaces (a) Ga rich surfaces (b) As(P) rich surfaces



(a)



(b)

Fig. 5. Work function values of clean surfaces and the surfaces after Cs adsorption (a) Ga rich surfaces  
(b) As(P) rich surfaces

Cs adsorption makes work function of GaAs<sub>0.5</sub>P<sub>0.5</sub>(001) reconstruction surfaces descend significantly regardless of As(P) rich or Ga rich condition. Nevertheless, it can be found that the work function decline amplitude of As(P) rich GaAs<sub>0.5</sub>P<sub>0.5</sub>(001) reconstruction surface is larger than that of Ga rich surface. The average work function variation of the two reconstruction surfaces are 1.093 eV and 1.829 eV, respectively. Cs atom adsorption on D<sub>2</sub> of Ga rich surface and D<sub>2'</sub> on As(P) rich surface makes the work function values of the two reconstruction surfaces reach minimums, which are 2.834 eV and 2.859 eV, respectively. From Fig. 1(b) and (d), it can be known that the  $\beta_2(4\times 2)$  and  $\beta_2(2\times 4)$  reconstruction surfaces are not flat due to the removal of a pair of Ga atoms or As(P) atoms. According to the height along [001] direction, the adsorption sites on Ga rich reconstruction surface can be classified into two groups: T<sub>1</sub>, D<sub>2</sub>, T<sub>5</sub>, T<sub>7</sub> on the topmost layer and D<sub>3</sub>, T<sub>4</sub>, T<sub>6</sub>, T<sub>8</sub> in the trenches. Obviously, Cs adsorption on the sites of first group makes greater decline. Similarly, the work function values of As(P) rich surfaces with Cs adsorption on topmost layer (T<sub>1'</sub>, D<sub>2'</sub>, T<sub>5'</sub>) are relatively smaller than those of surfaces with Cs adsorbed in trenches (D<sub>3'</sub>, T<sub>4'</sub>, T<sub>6'</sub>). However, there is no remarkable conclusion obtained by comparing dimer sites with and top sites.

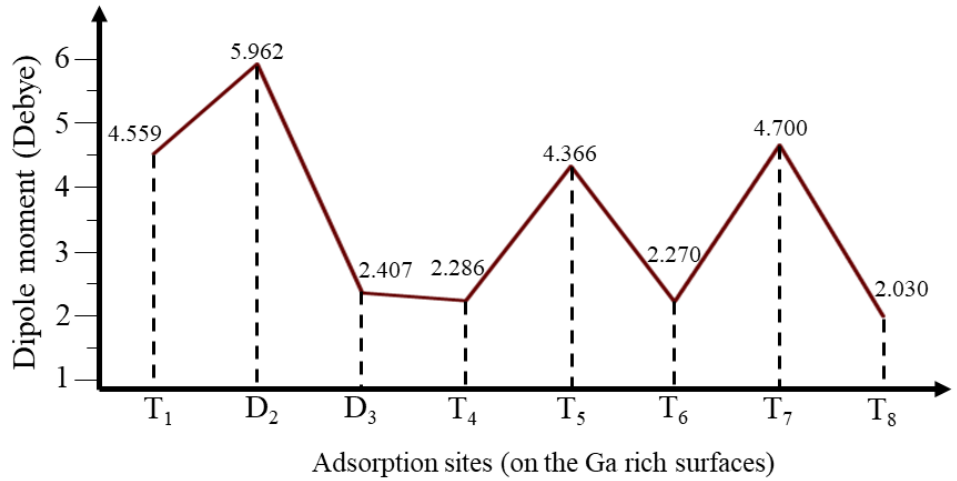
When Cs atoms adsorb on GaAs<sub>0.5</sub>P<sub>0.5</sub>(001) surface, Cs atoms gain positive charge while atoms in the GaAs<sub>0.5</sub>P<sub>0.5</sub> substrate obtain electrons, so Cs atoms interact with the substrate and establish dipole moments. Usually the direction of the dipole moment is not exactly orthogonal to the surface, and the intensity of the projection of the dipole moment on the [001] direction determines the value of the difference of the work function.

With the application of the Helmholtz equation, the surface dipole moment in Debye can be calculated with the following formula<sup>[27]</sup>:

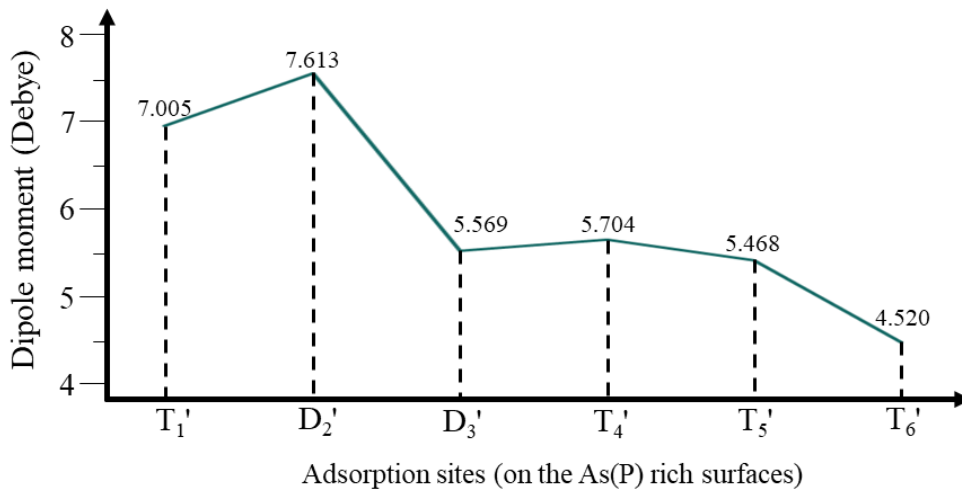
$$\mu = \frac{1}{12\pi} \frac{A\Delta\Phi}{\Theta} \quad (8)$$

where  $\Delta\Phi$  equals to the work function difference of clean surface and the surface with adsorption adatoms,  $A$  stands for the area in  $\text{\AA}^2$ , and  $\Theta$  represents the coverage of Cs adatom on the clean surface.

The calculated surface dipole moment is shown in Fig. 6. Since the coverage of Cs adatom for all adsorption sites is an equal and certain value, and the area of unit cell is constant at the same time, the surface dipole moment is only determined by  $\Delta\Phi$ , indicating  $\mu$  is linear in  $\Delta\Phi$ . As a result, the intensities of surface dipole moment on topmost layer are relatively larger than those of surfaces with Cs adsorbed in trenches.



(a)



(b)

Fig. 6. Surface dipole moments of the two reconstruction surfaces (a) Ga rich surfaces (b) As(P) rich surfaces

As work functions of Ga rich and As(P) rich surfaces reach the minimums when Cs is located at D<sub>2</sub> or D<sub>2</sub>', so the two adsorption models were selected to launch the following analysis on the atomic and electronic structures. After geometry relaxation the Cs adatom

at  $D_2$  is 3.465 Å higher than the outermost Ga atoms while Cs adatom at  $D_2'$  is 3.273 Å higher than the outermost As(P) atoms. And the thicknesses of bilayers and distance between bilayers for both Cs adsorbed models are shown in Table 4. It can be found that Cs adsorption does not affect the thicknesses of bilayers obviously, because the coverage of Cs atom is not very high.

Table 4. Thicknesses of bilyaers and distances between bilayers of Ga rich and As(P) rich surfaces after Cs adsorption

Layer	Cs adsorption			
	Thickness / Distance (Å)			
	Ga rich surface		As(P) rich surface	
	After Cs adsorption	variation	After Cs adsorption	variation
$D_1$	0.924	0.016	1.955	0.066
$d_{12}$	1.118	-0.016	0.876	-0.048
$D_2$	1.637	-0.033	1.751	0.006
$d_{23}$	1.366	0.015	1.182	-0.002
$D_3$	1.439	-0.007	1.539	-0.001

For Ga rich surface, the bond-length difference of the topmost bilayer between the clean surface and the Cs adsorption model ranges from -0.001 Å to -0.037 Å. The maximum change is located at the Ga atom of  $D_2$  and the As atom next to it. Both Ga dimers on the topmost layer got slightly extended. The change of the bond-length of the As atom and the P atom in the top bilayer and the two Ga atoms which are close to the top dimer at the edge of the pit on the second bilayer all reach over 0.01 Å. However, the dimer in the trench got shrank by 0.020 Å. There is no obvious shift for the atoms in lower layers.

For As(P) rich surface, the bond-length difference of the topmost bilayer between the clean surface and the Cs adsorption model ranges from 0.003 Å to 0.024 Å. The maximum change is located at the As atom and the P atom of  $D_2'$ . It is reasonable that the maximum change for both types of reconstruction surfaces is located at the atoms closest to the adsorption sites. Fig. 7 shows some detailed difference between the clean surface and  $D_2'$  adsorption model with a side view of the surface. The red rectangles contain all the bonds inside the rectangle area on the  $[\bar{1}10]$  direction, and therefore  $\overline{\Delta L_1}$ ,  $\overline{\Delta L_2}$ , etc. represent

the average difference of the certain bonds on the clean surface and on the surface with Cs adsorption. It can be learnt from Fig. 7 that the change of the bond-length of the dimer atoms and two lower Ga atoms which is closer to  $T_1'$  is bigger than that of which is on the other side. However, overall significant bond-length change occurs between the Ga atoms in the top bilayer and the As atoms in the second bilayer. The Ga atom between the dimers in the topmost layer and in the trench shifts remarkably, making the bond-length between the Ga atom and the lower As atom and P atom decrease over 0.03 Å.

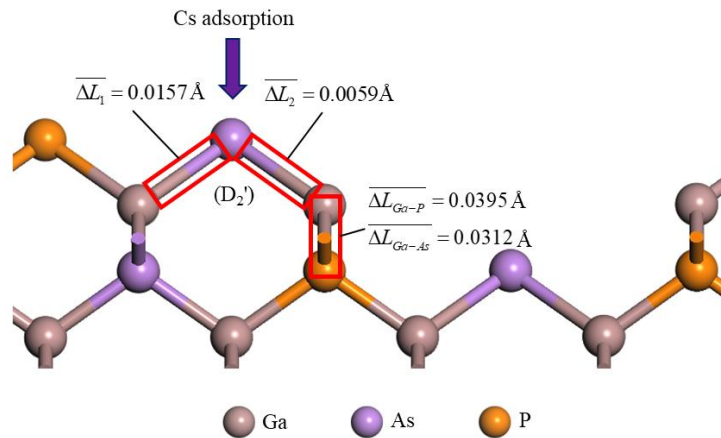


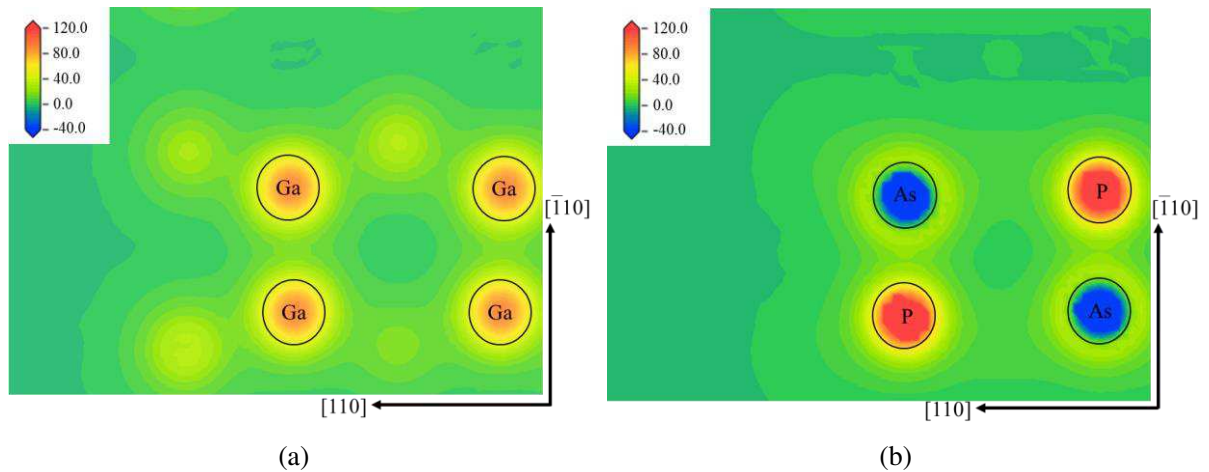
Fig. 7. Bond-length change of the  $D_2'$  Cs adsorption model

After Cs adsorption, the Mulliken charge population of the two surface models are shown in Table 5. The Cs adatoms at  $D_2$  and  $D_2'$  are 0.83 and 0.88, respectively, showing that adatoms transfer electrons to bulk atoms. According to Mulliken charge distribution, cations in the topmost layer of Ga rich surface and anions in the topmost layer of As(P) rich surface make the most contribution in obtaining electrons. For Ga rich surface, electrons in 3p state of the Ga atoms in the upmost monolayer increased and the charge of the atoms all dropped as a result of that, two of which even dropped to negative, from 0.08 and 0.07 to -0.08 and -0.09, respectively. While the electrons of the Ga atoms in the second layer did not change as much as those in the topmost layer, still generally dropped. The atoms of next two lower layer did not seem to be influenced, but the electron in s state of the atoms at the bottom declined. For the As rich surface, electrons of the atoms in the topmost bilayer changed most remarkably. To be exact, electrons in 4s state of the four Ga atoms below  $D_2'$  declined and electrons in 3p state of the P atom and 4p state of As atoms in the upmost monolayer rise, thus letting Ga and P atoms gain negative charge.

Nevertheless, electrons of the atoms in lower layers were not significantly affected. To display charge difference visually, charge difference maps of the topmost layer in Ga rich and As(P) rich reconstruction surfaces before and after Cs adsorption are shown in Fig. 8. Electron density of As(P) rich reconstruction surface is significantly larger than that of Ga rich surface. After Cs adsorption, electron density of the atoms in the topmost layer of both surfaces increase.

Table 5. Mulliken charge distribution of Ga rich and As(P) rich reconstruction surfaces after Cs adsorption

adsorption							
Ga rich reconstruction surface				As(P) rich reconstruction surface			
Atom	Total	Charge	$\Delta q$	Atom	Total	Charge	$\Delta q$
Ga <sub>1</sub>	12.96	0.04	-0.04	As <sub>1</sub>	5.19	-0.19	-0.07
Ga <sub>2</sub>	13.08	-0.08	-0.16	As <sub>2</sub>	5.26	-0.26	-0.14
Ga <sub>3</sub>	13.09	-0.09	-0.16	P <sub>1</sub>	5.32	-0.32	-0.05
Ga <sub>4</sub>	12.95	0.05	-0.03	P <sub>2</sub>	5.45	-0.45	-0.18
P <sub>1</sub>	5.40	-0.40	0.01	Ga <sub>1</sub>	12.89	0.12	0.06
P <sub>2</sub>	5.38	-0.38	0	Ga <sub>2</sub>	12.82	0.18	0.02
P <sub>3</sub>	5.38	-0.38	0	Ga <sub>3</sub>	12.87	0.13	0.07
As <sub>1</sub>	5.30	-0.30	-0.04	Ga <sub>4</sub>	12.83	0.17	0.02
As <sub>2</sub>	5.29	-0.29	-0.02	Ga <sub>5</sub>	12.87	0.13	-0.02
As <sub>3</sub>	5.26	-0.26	0	Ga <sub>6</sub>	12.86	0.15	-0.02



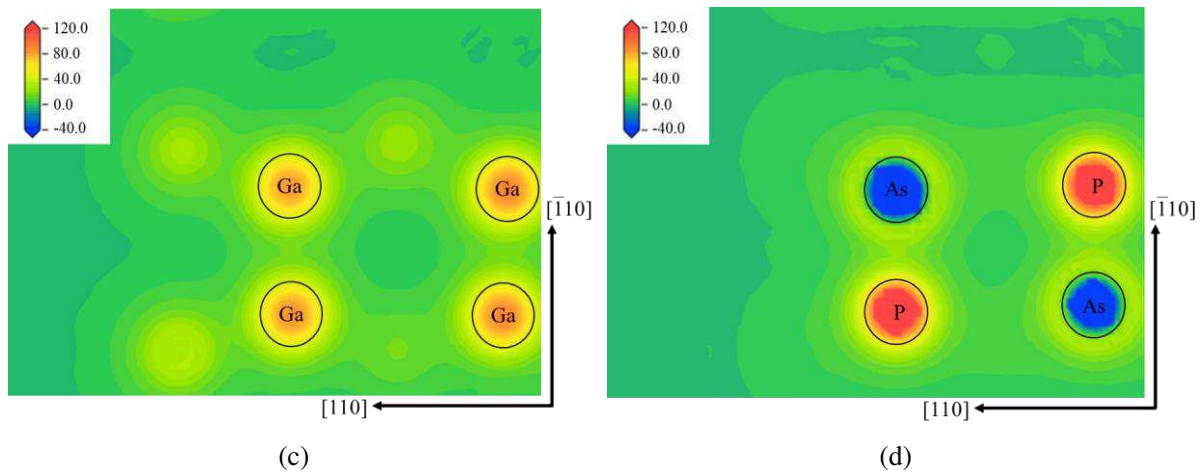


Fig. 8. Charge difference maps of the topmost layer of (a) Ga rich surfaces and (b) As(P) rich surfaces before Cs adsorption and (c) Ga rich surfaces and (d) As(P) rich surfaces after Cs adsorption

Based on the Mulliken distribution analysis, Cs adatoms with positive charges and the Ga, As, and P atoms obtaining electrons from Cs adatoms form dipole moments. So the overall dipole moment constitutes of many dipoles, which are formed by Cs-Ga, Cs-As, and Cs-P atoms. Besides, the quantities and directions of these decomposed dipole moments are different. And only the vector component perpendicular to  $[001]$  direction is beneficial for the decrease of work function. The schematic graphs of dipoles formed by Cs adatom and substrate atoms are shown in Fig. 9, in which Cs atoms adsorbed on the topmost layer (Fig. 9(a)) and in trenches (Fig. 9(b)), respectively. The indigo arrows present the dipoles formed by Cs adatoms and substrate atoms which are exactly under or approximately below the adatoms. So these dipoles have larger projection along  $[001]$  direction, thus they play more important roles in descending work function. Accordingly, the pink arrows in Fig. 9(a) present the dipole moments formed by Cs adatoms and substrate atoms in the trench while those in Fig. 9(b) stand for the dipole moments formed by Cs adatoms and substrate atoms in the topmost layers. In the first case, although the distance between Cs adatoms and substrate atoms is larger and the angle deviated from  $[001]$  direction is a little larger than that of the indigo arrows, they are helpful for lowering work function. In the second case, the pink arrows are approximately perpendicular to  $[001]$  direction, so they are not capable of lowering work function. What is more, in some models, there perhaps are some atoms in the topmost layer located higher than Cs atoms. As a result,

the dipoles have a detrimental effect on the overall dipole moments. So Cs adsorption on topmost layer is more effective than in the trenches.

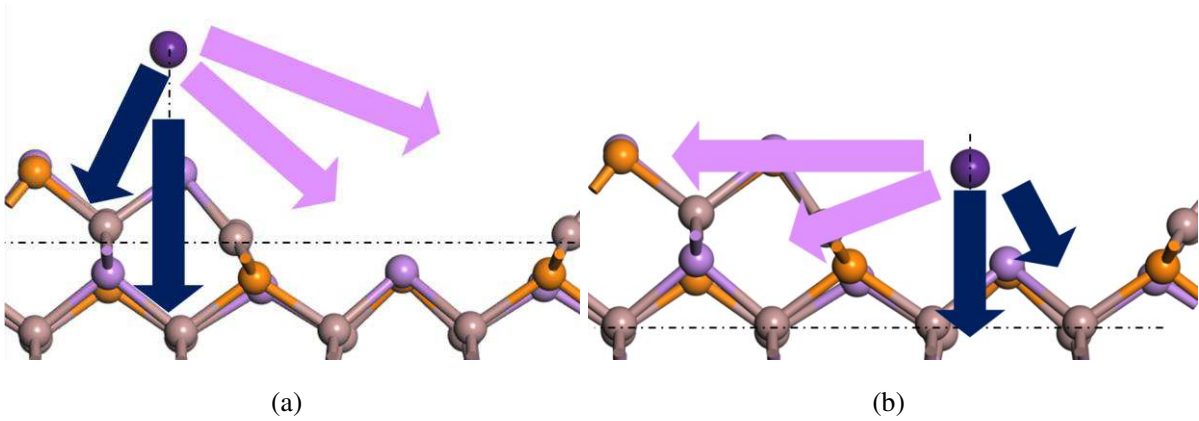


Fig. 9. Schematic graphs of dipoles formed by Cs adatom and substrate atoms (a) Cs adsorbed at  $D_2'$  (b) Cs adsorbed at  $T_6'$

As to the density of states, the PDOS of Cs adatom is shown in Fig. 10, and the TDOS of the surface before and after adsorption is shown in Fig. 11. From Fig. 10, it can be found that Cs-s state electrons appear at  $-25.5\sim-24\text{eV}$  and  $-0.5\sim 1\text{ eV}$  for Ga rich surface while they appear at  $-25\sim-23.5\text{eV}$  and  $0\sim 1\text{eV}$  for As(P) rich surface. Cs-s state electrons on Ga rich surface make more contribution at the Fermi level than those on As(P) rich one. From Fig. 11 it can be concluded that the TDOS curves of both models shifted to lower energy due to Cs adsorption, and the shifting effect is more obvious for As(P) rich surfaces.

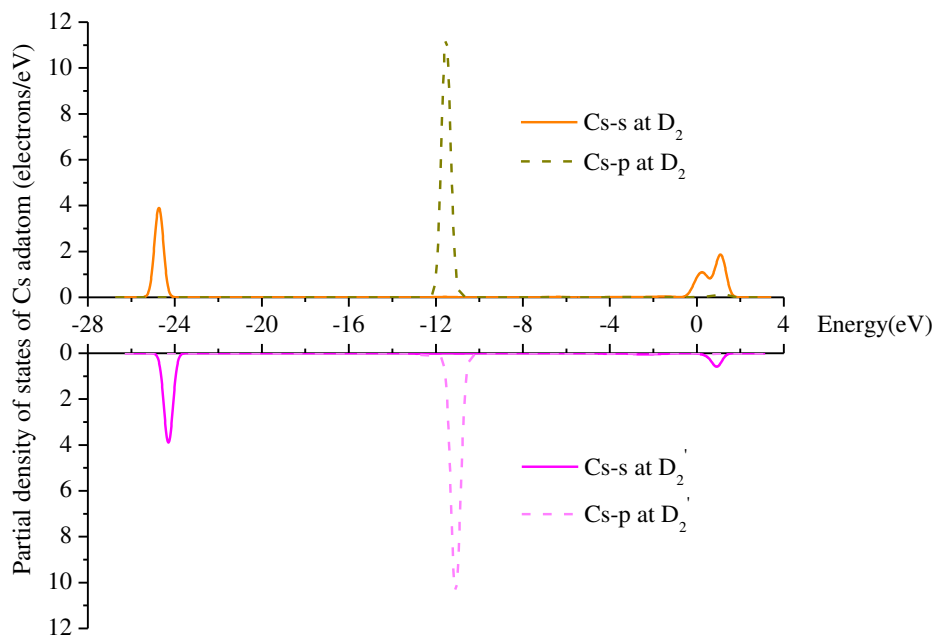


Fig. 10. PDOS curves of Cs adatom on D<sub>2</sub> and D<sub>2</sub>'

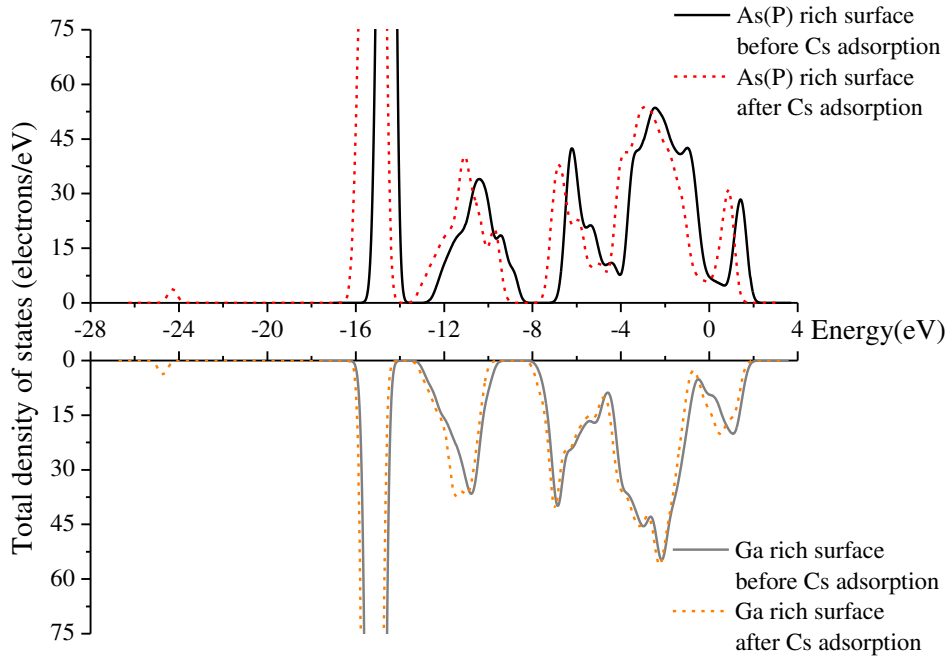


Fig. 11. TDOS curves before and after adsorption

#### 4. Conclusion

Atomic geometry and electronic structures of GaAs<sub>0.5</sub>P<sub>0.5</sub> (001) Ga rich  $\beta_2(4\times 2)$  and As(P) rich  $\beta_2(2\times 4)$  reconstruction surfaces with and without Cs adsorption were calculated by utilizing CASTEP software with first principle modeling method. Results indicate that GaAs<sub>0.5</sub>P<sub>0.5</sub> (001) Ga rich  $\beta_2(4\times 2)$  reconstruction surface has lower formation energy than As rich  $\beta_2(2\times 4)$  reconstruction surface. The work functions of two clean surfaces are 4.657 eV and 5.187 eV, respectively. Compared with bulk materials, the TDOS curves of both surfaces all shift to lower energy. In the Ga rich  $\beta_2(4\times 2)$  reconstruction surface, the Mulliken charge of Ga atoms in the topmost layer is significantly smaller than that of bulk Ga atoms. And in the As(P) rich  $\beta_2(2\times 4)$  reconstruction surface, the Mulliken charge of all atoms in the topmost layer is smaller than that of bulk atoms.

Cs adsorption helps the reconstruction surfaces lower their work functions, and the variation of the As(P) rich surface is more obvious than that of Ga rich surface. The work function minimums of Ga rich and As(P) rich surfaces are 2.834 eV and 2.859 eV, respectively. Coincidentally, the two minimums both occur when Cs adsorb on the dimer site of the topmost layer. Cs adatoms and substrate atoms form dipoles by transferring

electrons. According to Mulliken charge analysis, Cs atoms are positively charged and charge of substrate atoms descend after Cs adsorption. By calculating and analyzing dipole moments formed by Cs adatoms and substrate atoms, it can be found that Cs adsorption on the topmost layer is more effective in lowering work function than adsorption in trenches. As to the adsorption on the topmost dimer, Cs adatom gains a larger positive charge on the As(P) rich surface. After Cs adsorption, the TODS curve of As(P) rich surface shifts to lower energy more obviously than that of Ga rich surface.

## **Acknowledgment**

This study was funded by National Natural Science Foundation of China (Grant Nos. 61705108) and Natural Science Foundation of Jiangsu Province (Grant No. BK20170959). The authors acknowledge National Supercomputing Center in Shenzhen for providing the computational resources.

## **References**

- [1] Sadao, A.: Handbook on Physical Properties of Semiconductors, Volume 2, III-V Compound Semiconductors, Springer Science & Business Media, 2004
- [2] Yunus, O.: Characterization of Double-Junction GaAsP Two-Color LED Structure. *Journal of Electronic Materials*, 2018, 47(12): 7129-7133.
- [3] Konoreva, O.V.: The influence of acoustic-dislocation interaction on intensity of the bound exciton recombination in initial and irradiated GaAsP LEDs structures. *Superlattices and Microstructures*, 2017, 102: 88-93.
- [4] Gangcheng, J.: Comparison of blue-green response between transmission-mode GaAsP- and GaAs-based photocathodes grown by molecular beam epitaxy. *Chinese Physics B*, 2016, 25(4): 048505.
- [5] Xiuguang, J.: Picosecond electron bunches from GaAs/GaAsP strained superlattice photocathode. *Ultramicroscopy*, 2013, 130: 44-48.
- [6] <https://www.sbir.gov/sbirsearch/detail/201796>
- [7] Edgecumbe, J.P.: GaAsP photocathode with 40% QE at 550 nm. *SPIE*, 1992, 1655: 204-210.

- [8] Omar, S.: Nanoscale electrical analyses of axial-junction GaAsP nanowires for solar cell applications. *Nanotechnology*, 2020, 31(14): 145708.
- [9] Xinlong, C.: Quantum efficiency study of the sensitive to blue-green light transmission-mode GaAlAs photocathode, *Optics Communications*. 2015, 335: 42-47.
- [10] Xiaohua, Y.: Study on the electron structure and optical properties of Ga<sub>0.5</sub>Al<sub>0.5</sub>As(100)  $\beta_2(2\times 4)$  reconstruction surface. *Applied Surface Science*, 2013, 266: 380–385.
- [11] Schmidt, W.G.: III-V compound semiconductor (001) surfaces. *Applied Physics A*, 2002, 75: 89-99.
- [12] Schmidt, W.G.: Surface phase diagram of (2 $\times$ 4) and (4 $\times$ 2) reconstructions of GaAs(001), *Physical Review B*, 2000, 62: 8087-8091.
- [13] Northrup, J. E.: Energetics of GaAs(100)-(2 $\times$ 4) and-(4 $\times$ 2) Reconstructions, *Physical Review Letters*, 1993, 71: 2276-2279.
- [14] Kul'kova, S.E.: Atomic and Electron Structure of the GaAs (001) Surface, *Semiconductor Structures, Interfaces, and Surfaces 2007*, 41(7): 810-817.
- [15] Paget, D.: X-ray diffraction analysis of the gallium-rich surface of GaAs(001), *Physical Review B*, 2001, 64: 161305
- [16] Fukuda, Y.: H<sub>2</sub>S treated GaP(001) surface studied by low energy electron diffraction, Auger electron spectroscopy, and x ray photoelectron spectroscopy, *Applied Physics Letters*, 1992, 61: 955.
- [17] Sanada, N.: Clean GaP(001)-(4 $\times$ 2) and H<sub>2</sub>S-treated (1 $\times$ 2) S surface structures studied by scanning tunneling microscopy, *Applied Physics Letters*, 1995, 67: 1432.
- [18] Frisch, A.M.: (2 $\times$ 4) GaP(001) surface: Atomic structure and optical anisotropy, *Physical Review B*, 1999, 60: 2488.
- [19] Segall, M.D.: First-principles simulation: ideas. illustrations and the CASTEP code, *Journal of Physics: Condensed Matter*, 2002, 14: 2717–2744.
- [20] Perdew, J.P.: Generalized Gradient Approximation Made Simple, *Physical Review Letters*, 1996, 77: 3865.
- [21] Perdew, J.P.: Self-interaction correction to density-functional approximations for many-electron systems, *Physical Review B*, 1981, 23: 5048.
- [22] Monkhorst, H.J.: Special points for Brillouin-zone integrations, *Physical Review B*,

1976, 13: 5188.

[23] Xiaohua, Y.: Study on the electron structure and optical properties of GaAl<sub>0.5</sub>As<sub>0.5</sub> (100)  $\beta_2(2\times 4)$  reconstruction surface, *Applied Surface Science*, 2013, 266: 380-385.

[24] Rosa, A.L.: First-principles calculations of the structural and electronic properties of clean GaN (0001) surfaces. *Physical Review B*, 2006, 73(20): 205346

[25] Tasker, P. W.: The stability of ionic crystal surfaces. *Journal of Physics C: Solid State Physics*, 1979, 12(22): 4977-4984

[26] Sun, L.H.: Influences of Ca doping and Oxygen vacancy upon adsorption of CO on the LaFeO<sub>3</sub>(010) surface: A first-principles study, *The Journal of Physical Chemistry*, 2011, 115: 5593-5598.

[27] Wei-Xue L.: Oxygen adsorption on Ag(111): A density-functional theory investigation. *Physical Review B*, 2002, 65: 075407

# Figures

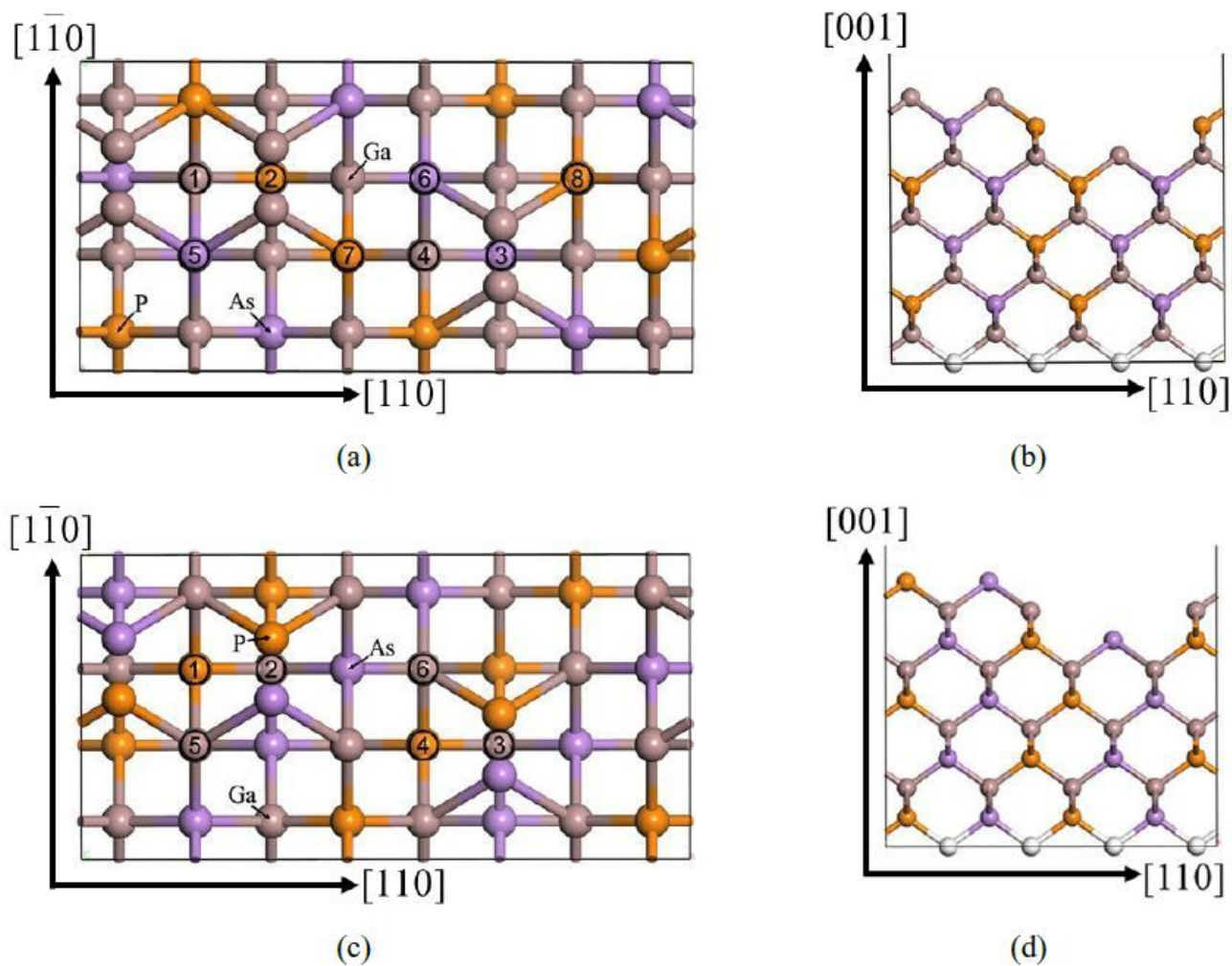


**Figure 1**

$\text{GaAs}_{0.5}\text{P}_{0.5}(001)$  reconstruction surfaces (a) top view of Ga rich  $\text{GaAs}_{0.5}\text{P}_{0.5}(001)$   $\beta_2(4 \times 2)$  (b) side view of Ga rich  $\text{GaAs}_{0.5}\text{P}_{0.5}(001)$   $\beta_2(4 \times 2)$  (c) top view of As(P) rich  $\text{GaAs}_{0.5}\text{P}_{0.5}(001)$   $\beta_2(2 \times 4)$  (d) side view of As(P) rich  $\text{GaAs}_{0.5}\text{P}_{0.5}(001)$   $\beta_2(2 \times 4)$

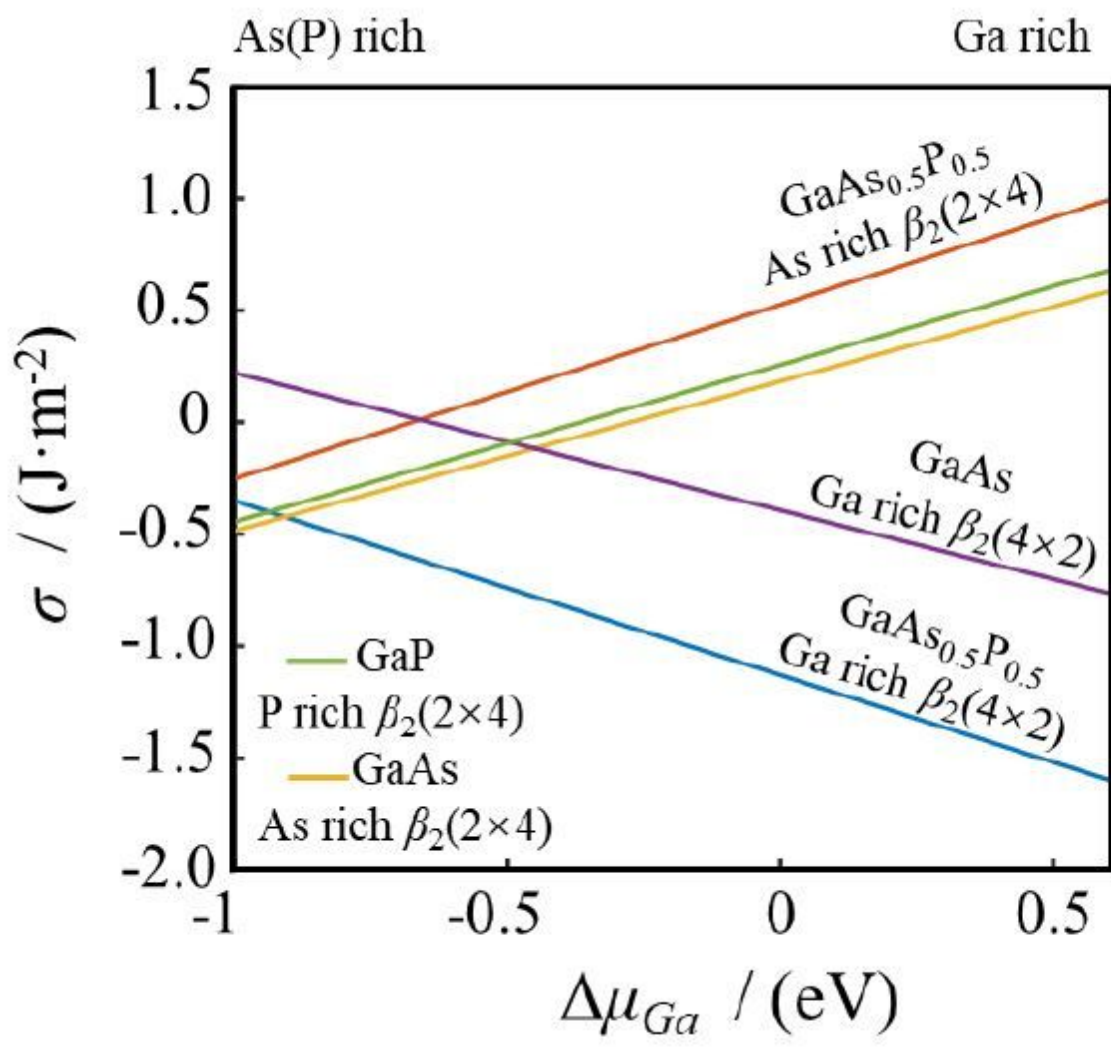
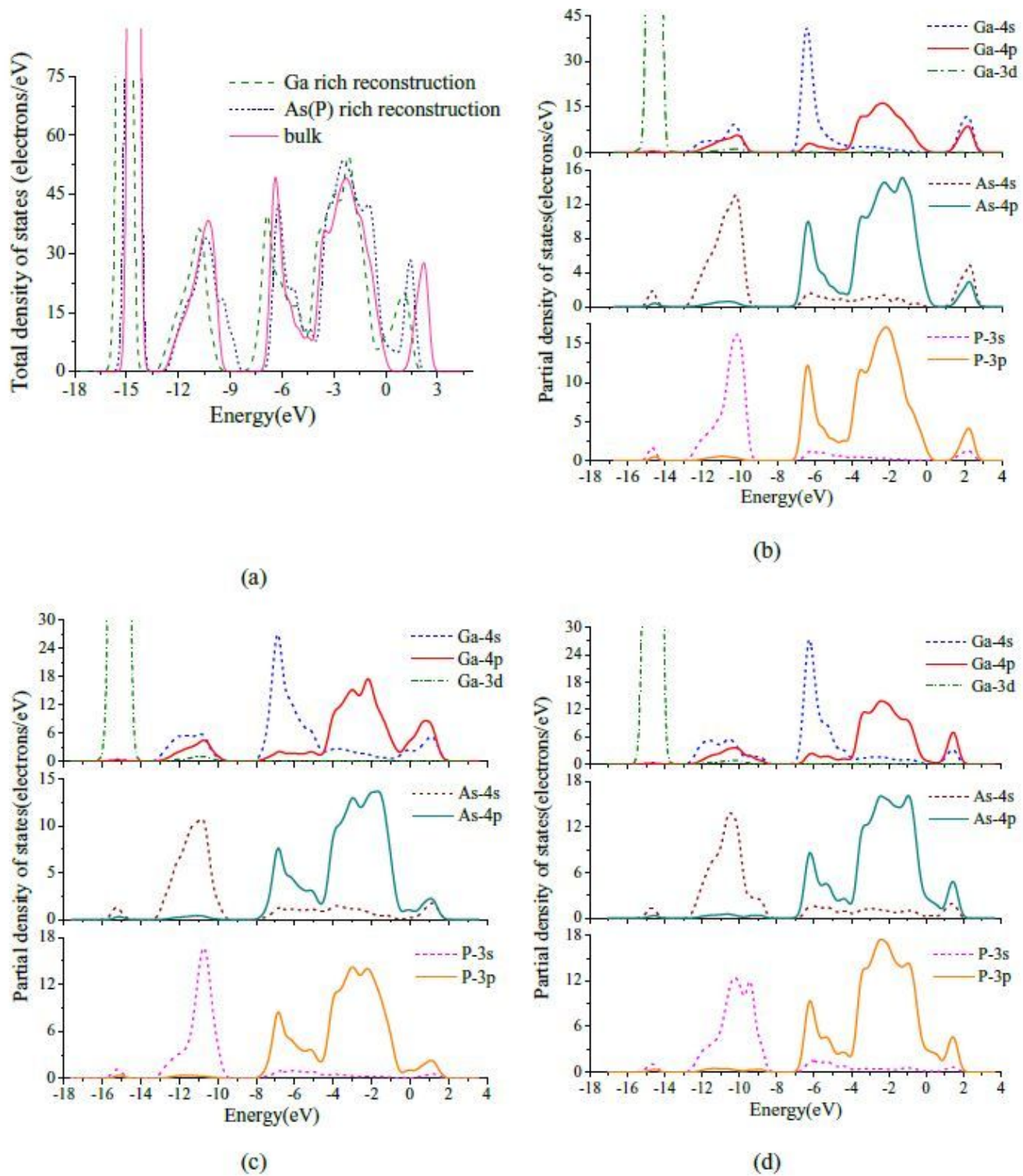


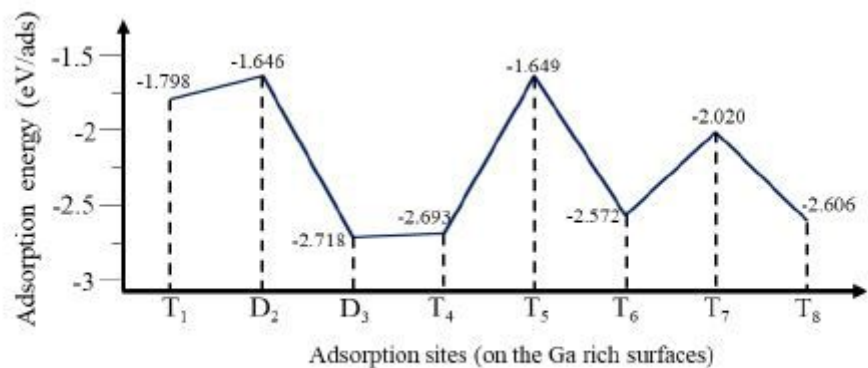
Figure 2

Formation energy curves of GaAs<sub>0.5</sub>P<sub>0.5</sub>(001) reconstruction surfaces

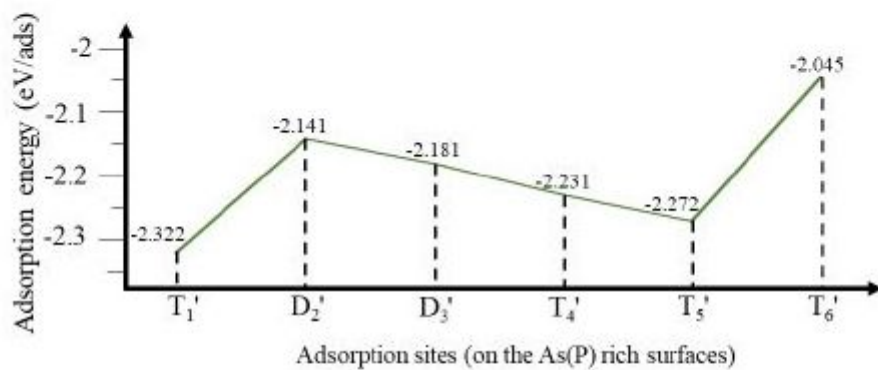


**Figure 3**

TDOS and PDOS of GaAs<sub>0.5</sub>P<sub>0.5</sub> bulk and GaAs<sub>0.5</sub>P<sub>0.5</sub>(001) reconstruction surfaces (a) TDOS curves of GaAs<sub>0.5</sub>P<sub>0.5</sub> bulk and GaAs<sub>0.5</sub>P<sub>0.5</sub>(001) reconstruction surfaces (b) PDOS curves of GaAs<sub>0.5</sub>P<sub>0.5</sub> bulk (c) PDOS curves of Ga rich GaAs<sub>0.5</sub>P<sub>0.5</sub>(001)  $\beta_2(4 \times 2)$  (d) PDOS curves of As(P) rich GaAs<sub>0.5</sub>P<sub>0.5</sub>(001)  $\beta_2(2 \times 4)$



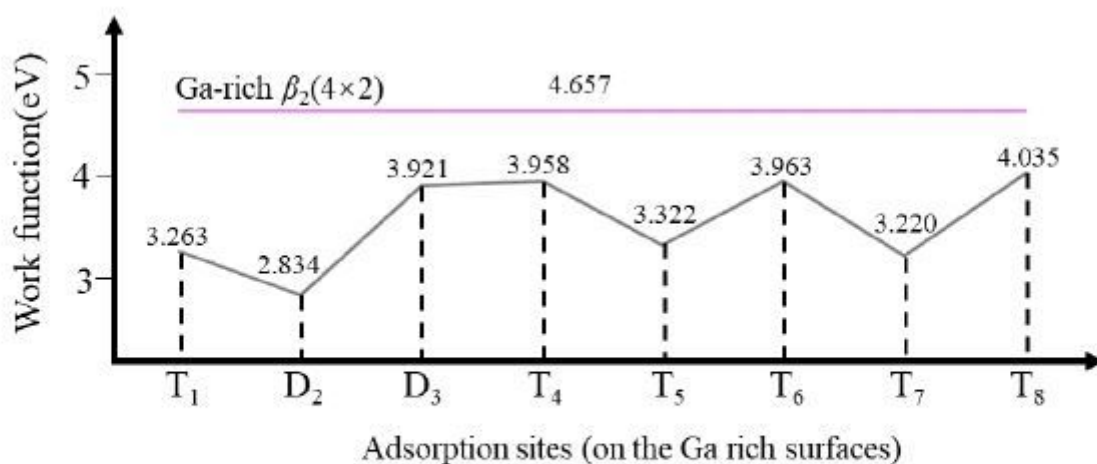
(a)



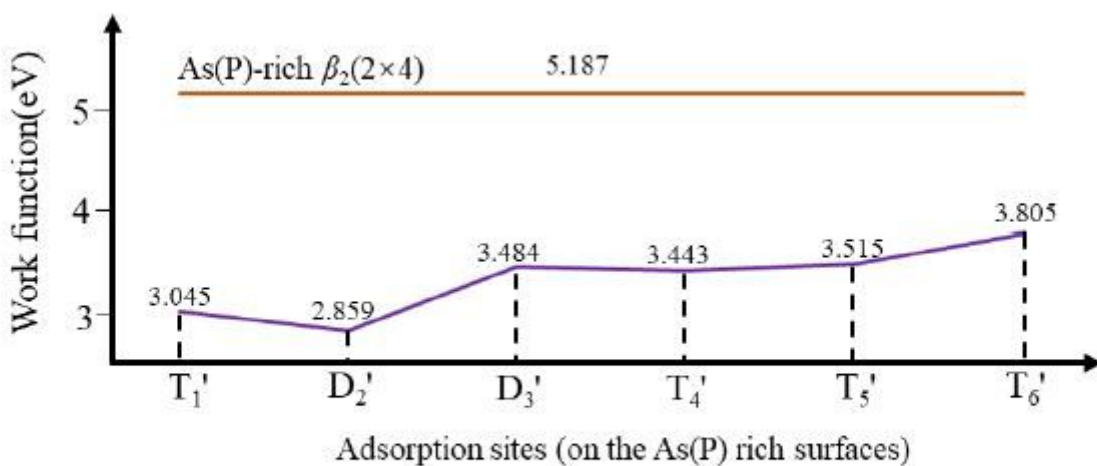
(b)

**Figure 4**

Cs adsorption energies of the two reconstruction surfaces (a) Ga rich surfaces (b) As(P) rich surfaces



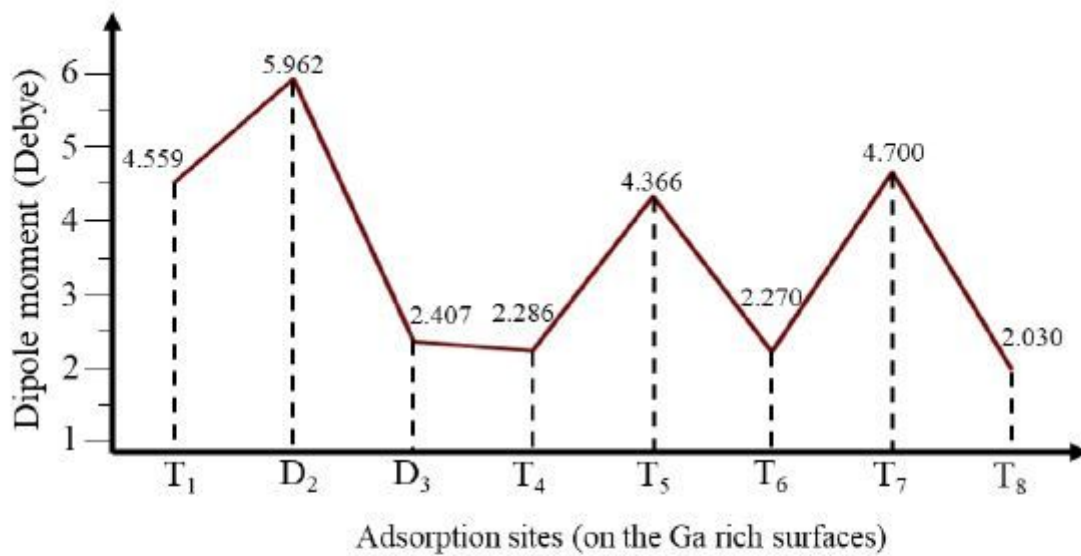
(a)



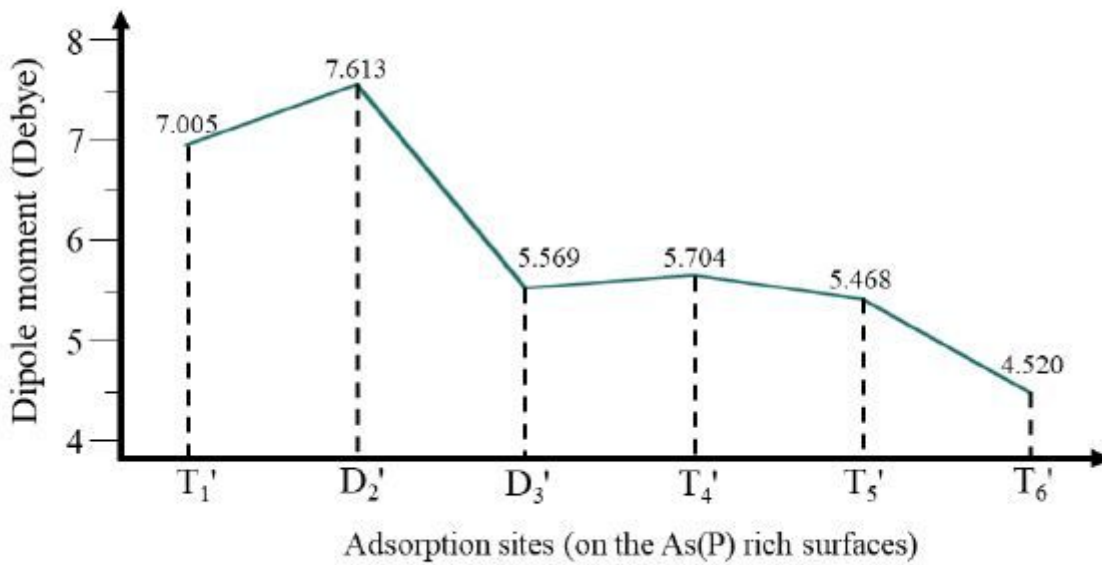
(b)

**Figure 5**

Work function values of clean surfaces and the surfaces after Cs adsorption (a) Ga rich surfaces (b) As(P) rich surfaces



(a)



(b)

Figure 6

Surface dipole moments of the two reconstruction surfaces (a) Ga rich surfaces (b) As(P) rich surfaces

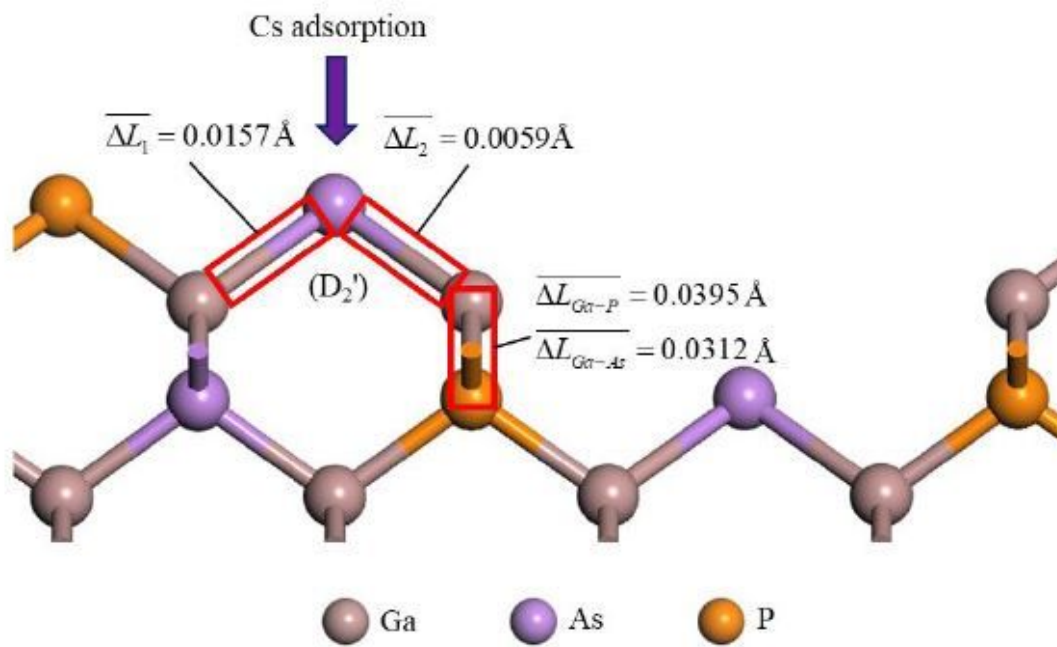
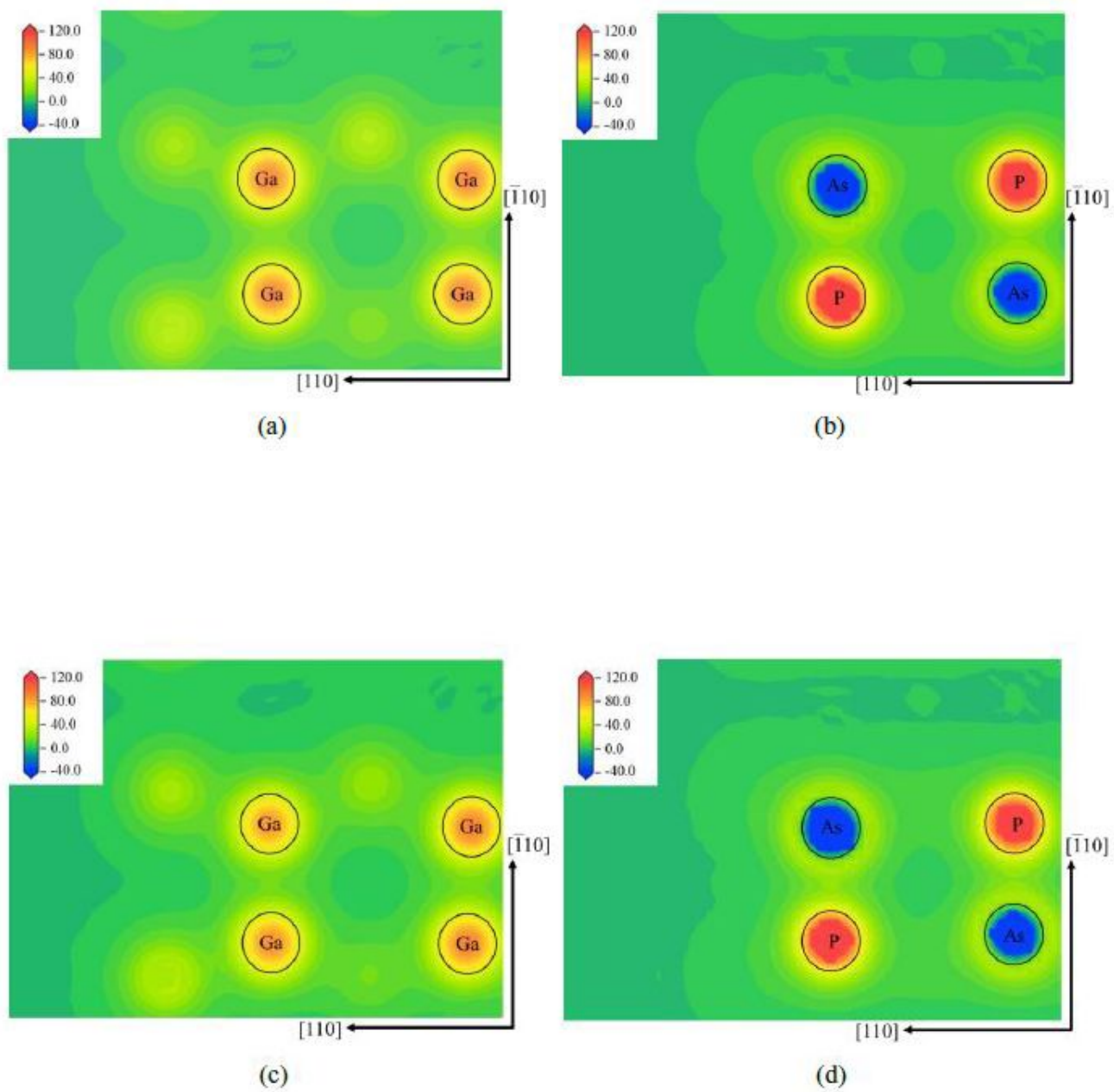


Figure 7

Bond-length change of the D<sub>2</sub>' Cs adsorption model



**Figure 8**

Charge difference maps of the topmost layer of (a) Ga rich surfaces and (b) As(P) rich surfaces before Cs adsorption and (c) Ga rich surfaces and (d) As(P) rich surfaces after Cs adsorption

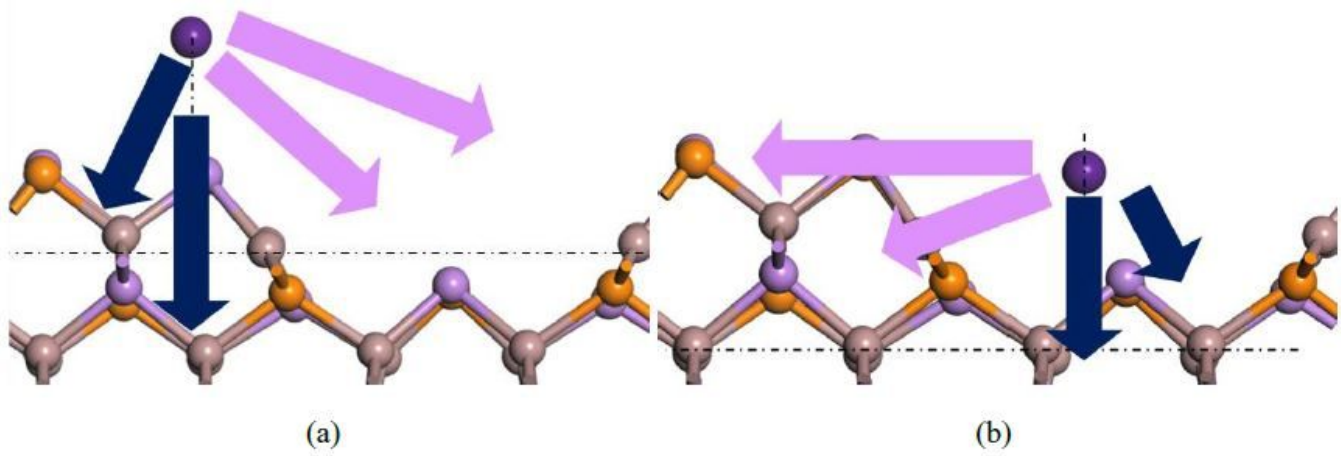


Figure 9

Schematic graphs of dipoles formed by Cs adatom and substrate atoms (a) Cs adsorbed at D2' (b) Cs adsorbed at T6'

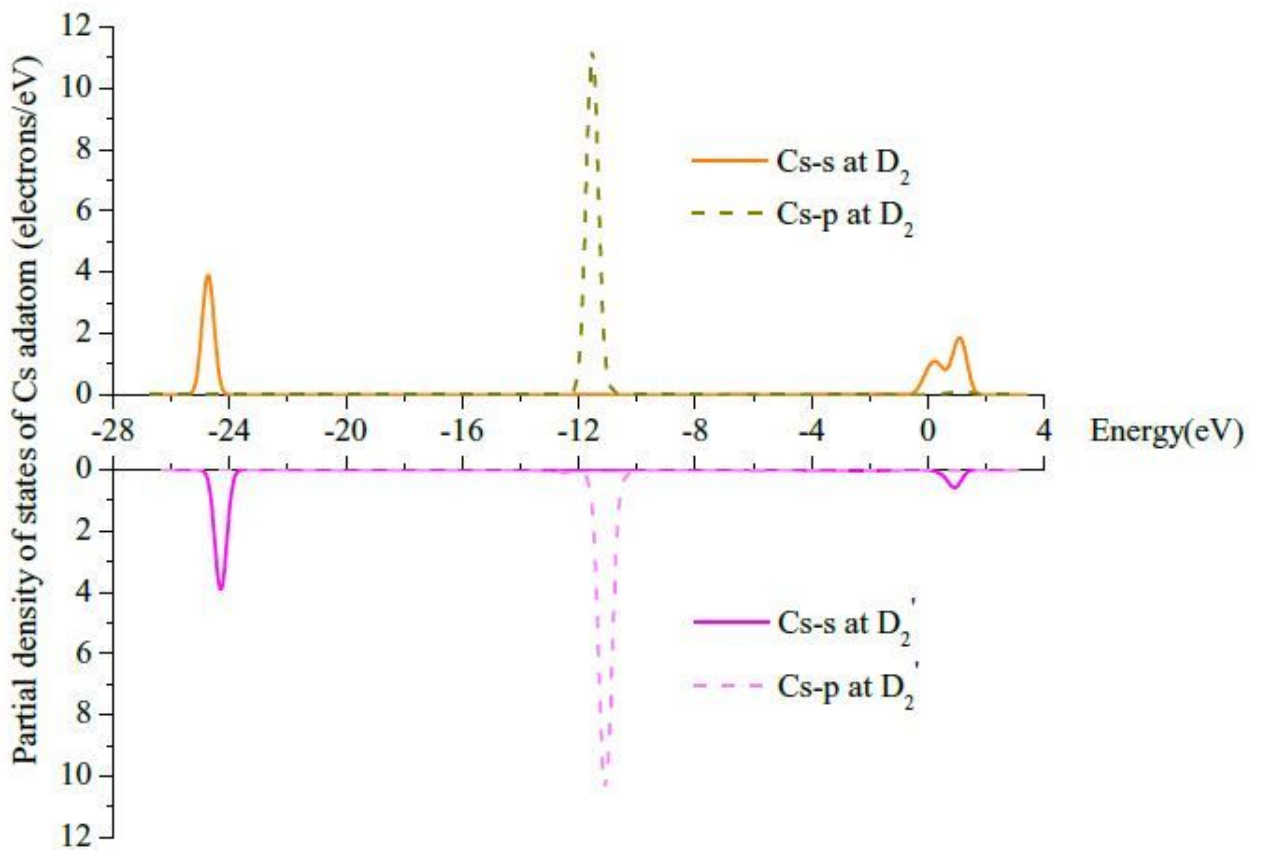
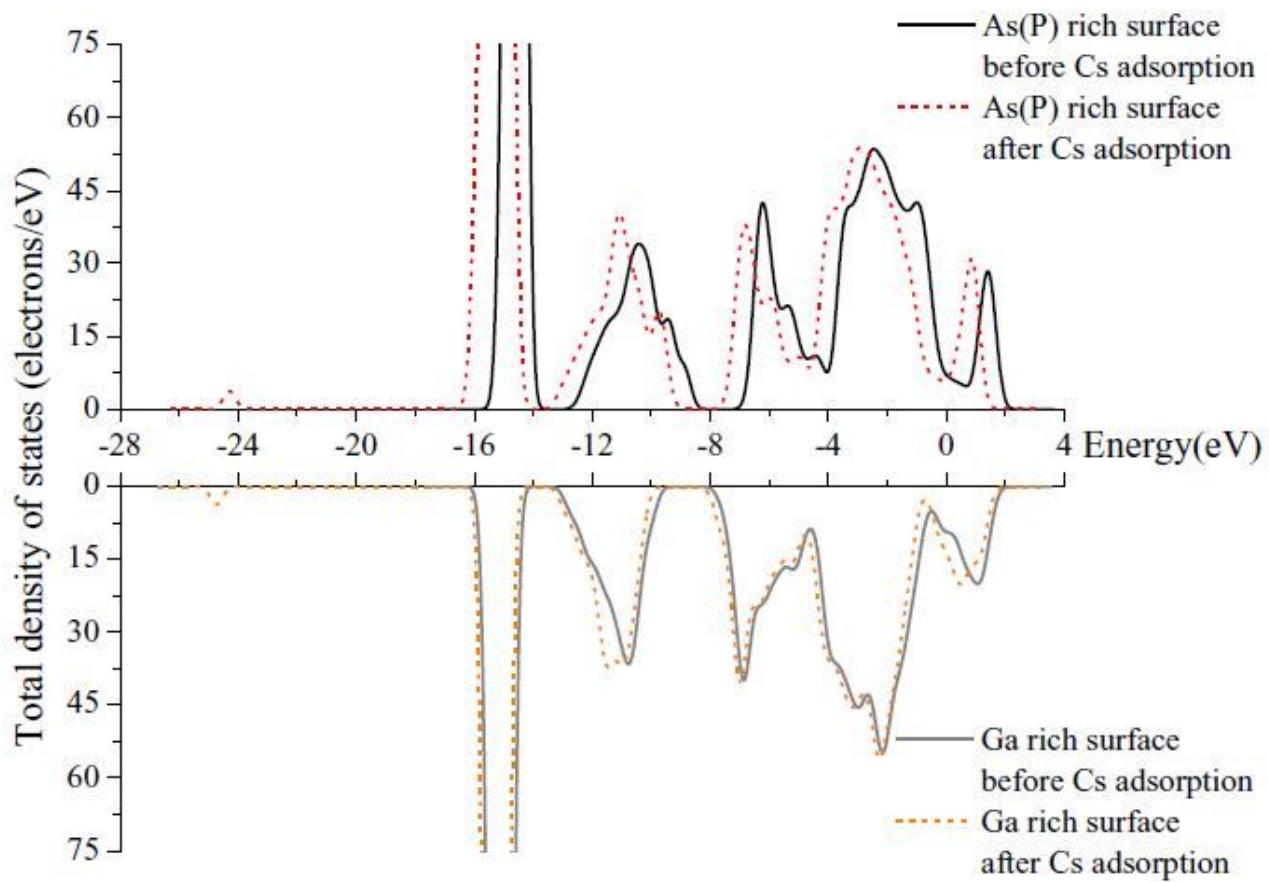


Figure 10

PDOS curves of Cs adatom on D2 and D2'



**Figure 11**

TDOS curves before and after adsorption